INTERNATIONAL JOURNAL OF CLIMATOLOGY
Int. J. Climatol. **33**: 2520–2541 (2013)
Published online 16 November 2012 in Wiley Online Library
(wileyonlinelibrary.com) DOI: 10.1002/joc.3606

RMetS
Royal Meteorological Society

A comparative assessment of monthly mean wind speed products over the global ocean

Elizabeth C. Kent,[a]* Susanne Fangohr[b] and David I. Berry[a]

[a] *National Oceanography Centre, Southampton, UK*
[b] *School of Ocean and Earth Science, University of Southampton, Southampton, UK*

ABSTRACT: The accurate estimation of marine wind speed is important for climate and air–sea interaction applications. There are many datasets of monthly mean wind speeds available based either on *in situ* measurements, satellite retrievals, atmospheric reanalysis assimilating both *in situ* and satellite data and blended datasets combining some or all of these other data sources. Twelve different monthly mean wind speed datasets are compared for the period from 1987 to 2009. The results suggest that we cannot presently be confident that the mean wind speed over the ocean is known to the accuracy required for the calculation of air–sea heat fluxes. Comparisons are complicated by different representations of wind speed being presented in different datasets. The *in situ* and reanalysis datasets present stability-dependent, earth-relative, wind speeds adjusted to a reference level of 10 m. The satellite and blended datasets present neutral equivalent, surface-relative, speeds adjusted to a reference level of 10 m. Differences between these estimates depend on atmospheric stability and ocean currents and can be greater than the required accuracy target. The adjustment for stability is itself uncertain but it is shown that these uncertainties are likely to be smaller than biases caused when the effects of stability are neglected. Further differences among the datasets are identified. Biases are caused by unidentified rain in K_u-band scatterometer-derived wind speeds and by atmospheric effects on passive microwave wind retrievals. When satellite observations affected by rain are removed a fair-weather bias remains. Some datasets are biased low in coastal regions by the effects of lower wind speeds over land in atmospheric models affecting wind speeds near the coast. All these uncertainties combine to give a wide range of estimates of monthly mean wind speed for the chosen datasets with uncertainty in mean values, spatial patterns and changes over time.

KEY WORDS wind speed; marine climatology; air–sea interaction; scatterometer; SSM/I; air–sea turbulent flux; air–sea CO_2 flux; structural uncertainty

Received 15 June 2012; Revised 6 September 2012; Accepted 25 September 2012

1. Introduction

Winds over the oceans regulate the coupling at the air–sea interface that maintains global and regional climate by modulating air–sea fluxes of heat, moisture and gases. The accepted benchmark for surface net heat flux accuracy is ± 10 W m^{-2} over monthly to seasonal time scales and a spatial scale of between 2° and 5° (Fairall *et al.*, 2010; WCRP, 1989; Webster and Lukas, 1992; WGASF, 2000; Weller *et al.*, 2004), implying determination of individual components of the net heat flux to a few W m^{-2}. Where turbulent fluxes are parameterized this sets limits on the mean bias of the input observations (Fairall *et al.*, 1996) of order 0.2 K for air and sea temperatures, 0.3 g kg^{-1} for humidity and 0.2 m s^{-1} for wind speed (Bradley and Fairall, 2007). Other applications, for example, global climate change or annual ice mass calculations, require even greater accuracy (Bourassa *et al.*, 2010).

Presently available sources of marine wind speed data all have limitations. *In situ* observations from ships are geographically limited and may be affected by biases including air flow distortion (Moat *et al.*, 2005). Random uncertainties in observations from Voluntary Observing Ships (VOS) are typically large (Kent *et al.*, 1998; Kent and Berry, 2005). Wind speeds from Research Vessels are sparse (Gould and Smith, 2006) and require careful analysis (Smith *et al.*, 1999). Measurements from moored meteorological buoys have the potential to be accurate (Gilhousen, 1987; Thomas *et al.*, 2005), but are geographically limited. Most buoys are located either in near-coastal regions in the northern hemisphere (Woodruff *et al.*, 2008) or in the Tropical arrays (McPhaden *et al.*, 1998, 2009; Bourlès *et al.*, 2008). There are considerable difficulties in making long-term measurements from buoys including proximity to the sea-surface, wave-induced buoy motions, sheltering in wave troughs and power limitations (Weller *et al.*, 2008). Satellite-borne instruments can acquire wind speed data with global coverage, high spatial resolution and frequent sampling (Bourassa *et al.*, 2010). However, there are significant differences between

* Correspondence to: Dr E. C. Kent, National Oceanography Centre, European Way, Southampton, SO14 3ZH, UK. E-mail: eck@noc.ac.uk
[The copyright line in this article was changed on 30 August 2014 after original online publication.]

winds measured from different types of satellite sensor that depend on the details of the measurement method.

There are many available gridded wind products, some combining data from several different sources. Some are available at high temporal and spatial resolution, but here we focus on monthly mean datasets of several years duration to assess their accuracy against the adequacy requirements for surface heat fluxes. We note that achieving the monthly mean accuracy of $0.2\,\mathrm{ms}^{-1}$ is a necessary but not sufficient requirement for achieving the desired accuracy in parameterized heat fluxes.

In this article, we compare 12 different sources of monthly mean wind speed data, from satellite scatterometers, satellite passive microwave, an *in situ* only product, atmospheric reanalysis and blended products combining wind data from different sources. We focus on the ability of the products to meet the accuracy requirements for the calculation of surface fluxes from mean meteorological observations. Section 2 describes surface fluxes and the calculation of gridded flux fields. The wind data products are introduced in Section 3. Section 4 presents results of the comparison of monthly mean wind products. Conclusions are drawn in Section 5.

2. Wind speed, turbulent fluxes and the atmospheric surface boundary layer

2.1. Wind speed and air–sea turbulent fluxes

Direct measurements of the turbulent heat fluxes are difficult and expensive to make, requiring continuous high frequency observations (Large and Pond, 1981) together with detailed information on the motion of the observing platform (Edson *et al.*, 1998) and the flow distortion over the platform (Yelland *et al.*, 2002). Long-term direct measurements of turbulent air–sea fluxes (Prytherch *et al.*, 2010) are rare. The difficulty of making these measurements means that the global ocean is extremely sparsely sampled with direct heat flux measurements and we must therefore appeal to flux parameterizations to produce global flux fields based on more frequently observed parameters. These parameters include wind speed, air–sea temperature difference, air–sea humidity difference and pressure. Other parameters such as sea state are also sometimes included (Bourassa *et al.*, 1999). Even these basic parameters are not uniformly sampled over the ocean and the use of satellite-derived wind speeds, which are relatively well sampled from space, is highly desirable.

Flux parameterizations, known as bulk formulae, model the turbulent exchange as a function of the surface atmospheric and oceanic states. On the basis of direct measurements of the fluxes made during dedicated research cruises, together with observations of the bulk meteorological variables, many different parameterizations have been developed for the turbulent fluxes (Liu *et al.*, 1979; Smith, 1980, 1988; Clayson *et al.*, 1996; Fairall *et al.*, 2003). The bulk formulae can be written:

$$\tau = -\rho_0 C_D\,(u_z - u_0)^2 \tag{1}$$

$$H_s = c_p\,\rho_0 C_H\,(u_z - u_0)\,(T_z - T_0) \tag{2}$$

$$H_l = \rho_0 L C_E\,(u_z - u_0)\,(q_z - q_0) \tag{3}$$

$$F_{\mathrm{gas}} = sk\,(pX_w - pX_a) \tag{4}$$

where τ is the wind stress ($\mathrm{N\,m}^{-2}$), ρ_0 is the density of air ($\mathrm{kg\,m}^{-3}$), C_D is the drag coefficient, u_z is the wind speed (ms^{-1}) at the observation height z (m), u_0 is the current speed in the direction of the wind vector (ms^{-1}), H_s is the sensible heat flux ($\mathrm{W\,m}^{-2}$), c_p is the specific heat capacity of air at constant pressure ($\mathrm{J\,kg\,K}^{-1}$), C_H is the transfer coefficient for sensible heat, T_z is the air temperature at the observation height (K), T_0 is the sea surface temperature (SST K), H_l is the latent heat flux ($\mathrm{W\,m}^{-2}$), L is the latent heat of vaporization ($\mathrm{J\,kg}^{-1}$), C_E is the transfer coefficient for latent heat, q_z is the specific humidity at the observation height ($\mathrm{kg\,kg}^{-1}$), q_0 is the specific humidity just above the sea surface (usually taken as the 98% saturation value at the SST, $\mathrm{kg\,kg}^{-1}$). F_{gas} is gas flux from ocean to atmosphere, s is the solubility of the gas in seawater at temperature T_0 and salinity S, k is the transfer velocity across the interface given in units of centimetres per hour and pX_w and pX_a are the partial pressures of gas on the sea and air side of the interface, respectively.

The transfer coefficients (C_D, C_H and C_E, Equations (1)–(3)) are all functions of the atmospheric stability and several iterations are required to obtain the wind stress and heat fluxes. The bulk formulae differ primarily in the form that is assumed for the neutral transfer coefficients and for the dimensionless stability parameters (WGASF, 2000; Brunke *et al.*, 2003). The transfer coefficients are strongly dependent on the atmospheric stability leading to a wide spread in the coefficients at low wind speeds. There is fairly good agreement about the form that the stability adjustments take, with most formulations varying only at the extremes of the stability range. There is less agreement about the neutral values of the transfer coefficients, especially at high wind speeds when direct flux measurements are rare (Brunke *et al.*, 2003; Prytherch *et al.*, 2010).

Parameterizations of gas transfer velocity of CO_2 commonly rely on wind speed (Wanninkhof, 1992; Nightingale *et al.*, 2000; Equation (4)) and vary between square and cubic functions of wind speed so nonlinear effects are particularly important (Wanninkhof *et al.*, 2002; Fangohr *et al.*, 2008). In an attempt to parameterise those surface processes that do not scale with wind speed, some more recent theoretical parameterizations of k also include a dependence on remotely sensed mean square slope, friction velocity and whitecapping (Glover *et al.*, 2002; Woolf, 2005; Fangohr and Woolf, 2007). However, lack of observations of these parameters collocated with direct flux measurements mean that wind-speed-based parameterizations remain in use (Prytherch *et al.*, 2010; Fairall *et al.*, 2011). A recent overview is given by Wanninkhof *et al.* (2009).

Ideally global flux fields would be calculated from high accuracy, high resolution, collocated observations of each of the input parameters to the bulk formulae. High quality collocated observations of the surface atmospheric and oceanic states are not frequent enough to allow the construction of global fields. It is obvious that biased input variables will lead to biased fluxes, but even normally distributed random errors with zero mean bias may lead to biased estimates of the fluxes due to the nonlinearity of the bulk formulae (Berry, 2009). This is most problematic for observations containing large random uncertainties. If fluxes are calculated from gridded estimates of the surface atmospheric and oceanic states then biases can arise if synoptic scale correlations between the different variables are not captured (Ledvina *et al.*, 1993; Josey *et al.*, 1995; Gulev, 1997). If the gridded estimates are derived from data sources that are not collocated then there is the potential for bias if the input fields for different variables are mismatched in time or resolve different scales of variability.

2.2. The adjustment of wind speed to a reference height and to neutral conditions

Near the surface of the ocean the wind speed typically decreases with height because of the drag exerted on the atmosphere by the ocean. The bulk formulae therefore require known height of measurement of wind speed and also of temperature and humidity that are needed to estimate the stability of the atmosphere near the ocean surface. An output from the flux calculation (Section 2.1, Equations (1)–(3)) is therefore the wind speed, temperature and humidity referenced to a standard height, usually 10 m. The gradient of wind speed with height depends on the atmospheric stability and is greater under stable conditions than unstable conditions. In the terminology used here winds as measured are 'stability-dependent'. Calculation of the height adjustment requires knowledge of the atmospheric stability to provide a stability-dependent estimate of 10 m wind speed (the wind speed that would have been measured if the sensor was actually at 10 m height). If the atmospheric stability is unknown (because collocated observations of T_0, T_z or q_z are missing) an approximate adjustment can be made assuming that the stratification of the atmosphere is neutral. This approach will provide an approximation to the stability-dependent 10 m wind speed, the bias in which will depend on the difference between the neutral and actual wind profile.

A further adjustment that can be applied is to calculate the equivalent neutral wind speed, again usually referenced to 10 m height. The equivalent neutral wind is the wind speed that in a neutral atmosphere would give rise to the same surface stress as the observed stability-dependent wind speed. Conceptually this means calculating the surface stress using the full stability-dependent calculation and then using this stress to calculate the wind that would have produced this particular value under neutral conditions. Because the near surface gradients are stronger under neutral conditions rather than unstable conditions normally observed over the ocean, the adjustment from stability-dependent to neutral equivalent wind speed is positive (neutral winds are stronger than measured wind speeds in unstable conditions). In the less-common stable conditions neutral winds are weaker than measured winds.

The adjustment of wind speeds for height and to give a neutral equivalent wind speed requires assumptions to be made about the expected structure of the near surface atmosphere. The framework for these assumptions is Monin-Obukhov similarity theory (MOST) that underpins the bulk formulae. Each different version of the bulk formula will therefore give different results due the different assumptions each makes about the relationships among surface roughness, stress and atmospheric stability. This is discussed further in Section 4.1. Details on how to make these adjustments can be found in Chapter 7 of WGASF (2000).

3. Datasets and data processing

3.1. The datasets used in this study

The 12 monthly mean marine wind speed datasets used in this study are all freely available and their characteristics are summarized in Table 1. There are however several notable datasets that have not been included. Two recent reanalysis products, the NASA Modern-Era Retrospective Analysis for Research and Applications (MERRA; Rienecker *et al.*, 2011) and the National Centers for Environmental Prediction (NCEP) Climate Forecast System Reanalysis (CFSR; Saha *et al.*, 2010), were not included because they do not provide monthly mean wind speed data. Previous versions of some of the datasets are compared by Wallcraft *et al.* (2009) and Smith *et al.* (2011).

3.1.1. European Remote Sensing Satellites 1 and 2 (ERS1 and ERS2; IFREMER/CERSAT, 2002a)

These datasets comprise C-band microwave scatterometer data from ERS1 and ERS2 as processed by the Center for Satellite Exploitation and Research (CERSAT) of the French Institute of Research for the Exploration of the Sea (IFREMER, IFREMER/CERSAT, 2002a). Over ice the retrieval is not related to wind speed and the anomalous backscatter over ice is used to provide an ice mask. Details of the land mask used are not given. Scatterometer wind values are neutral winds at a 10-m reference level. The nominal cell size for ERS scatterometer data is 50 km. The sensors have a single swath of 500 km requiring 3–4 days to provide global coverage.

The documentation (IFREMER/CERSAT, 2002a) notes that winds below 3.5 ms^{-1} are likely to be inaccurate. ERS scatterometers are expected to overestimate low wind speeds and underestimate high wind speeds. Ten-metre neutral winds between 3.5 and 15 ms^{-1}

Table 1. Summary of characteristics of monthly mean wind products compared in this study. All products are referenced to 10 m height. Note that not all input data sources listed are available for the full period of any particular dataset.

Product	Input wind data	Period	Grid	Stability
ERS1 http://cersat.ifremer.fr/Data/Discovery/By-product-type/Gridded-products/MWF-ERS IFREMER/CERSAT, 2002a	ERS1 scatterometer	August 1991 to May 1996	1° × 1°, 80°S–80°N	Neutral
ERS2 http://cersat.ifremer.fr/Data/Discovery/By-product-type/Gridded-products/MWF-ERS IFREMER/CERSAT, 2002a	ERS2 scatterometer	April 1996 to December 2000	1° × 1°, 80°S–80°N	Neutral
CERSAT QuikSCAT (QS_CERSAT) http://www.ifremer.fr/cersat/en/data/gridded.htm IFREMER/CERSAT, 2002b	QuikSCAT scatterometer	August 1999 to October 2009	0.5° × 0.5°, 80°S–80°N	Neutral
RSS v4 QuikSCAT (QS_RSS4), http://www.ssmi.com/qscat/qscat_description.html Ricciardulli and Wentz (2011)	QuikSCAT scatterometer	July 1999 to November 2009	0.25° × 0.25° 80°S–80°N	Neutral
HOAPSv3 http://www.hoaps.zmaw.de/ Andersson *et al.* (2007)	SSM/I	July 1989 to December 2005	0.5° × 0.5°, global	Neutral
NOCv2.0 http://www.noc.soton.ac.uk/noc_flux/noc2.php Berry and Kent (2009, 2011)	VOS	January 1973 to December 2009	1° × 1°, global ice-free	Stability-dependent
NCEP http://www.esrl.noaa.gov/psd/data/gridded/data.ncep.reanalysis.html Kalnay *et al.* (1996)	VOS, buoys	January 1948 to present	2.5° × 2.5°, global, including land	Stability-dependent
Twentieth Century Reanalysis (V2) http://www.esrl.noaa.gov/psd/data/20thC_Rean/ Compo *et al.* (2011)	none	January 1871 to December 2010	2° × 2°, global, including land	Stability-dependent
ERAI http://data.ecmwf.int/data/ ECMWF (2007); Uppala *et al.* (2008a, 2008b); *Dee et al.* (2011)	VOS, buoys, SSM/I and ERS1&2 scatterometers, QuikSCAT (post March 2000)	January 1989 to present	1.5° × 1.5°, global, including land	Stability-dependent
BSW http://www.ncdc.noaa.gov/oa/rsad/seawinds.html Zhang *et al.* (2006a, 2006b)	SSM/I, AMSR-E, TMI, QuikSCAT, plus directions from NCEP/DOE2	July 1987 to present	0.25° × 0.25°, global	Neutral
CCMP v1.1, Level 3.5a, fast look http://podaac.jpl.nasa.gov/datasetlist Atlas *et al.* (2011)	SSM/I, AMSR-E, TRMM TMI, QuikSCAT, VOS, buoys, ERA40 and ECMWF Operational Analysis	July 1987 to December 2009	0.25° × 0.25°, global	Neutral
OAFlux http://oaflux.whoi.edu/ Yu and Weller (2007); Yu *et al.* (2008)	NCEP, NCEP2, ERA40, SSMI, QuikSCAT, AMSR-E	January 1958 to December 2009	1° × 1°, global	Neutral

were thought to be without significant bias (IFREMER/CERSAT, 2002a). Documentation of the European Space Agency's (ESA) current Advanced Scatterometer (ASCAT; Verhoef and Stoffelen, 2011) indicates a low bias in ERS1 and ERS2 of 0.5 ms^{-1} relative to buoy winds at all wind speeds.

In order to reconstruct gap-filled fields from discrete observations a statistical interpolation is performed using an objective method; the standard errors of the parameters estimated by this method are also computed and provided (IFREMER/CERSAT, 2002a). It is not clear from the documentation which combination of data quality flag values has been used to generate the monthly mean product.

3.1.2. NASA SeaWinds scatterometer (QuikSCAT: QS_CERSAT, QS_RSS4)

The SeaWinds scatterometer aboard QuikSCAT provided twice-daily near-global coverage from 1999 to 2009 with a swath width of 1800 km. The Jet Propulsion Laboratory (JPL) and Remote Sensing Systems (RSS) have each produced their own level 2b (swath) and level 3 (gridded) wind data since the launch of the instrument. Whilst generally consistent with each other, the datasets are based on different geophysical model functions

that relate sea-surface roughness to wind and subtle differences exist (Fangohr and Kent, 2012). In April 2011, RSS reprocessed their entire data from version 3.0 to version 4.0 reducing some of the more substantial discrepancies at high wind speeds. Differences remain but are expected to be small on large spatio-temporal scales. Two different monthly mean datasets of QuikSCAT observations are used in this study. The first uses wind vectors produced by the JPL processed to give monthly mean wind speeds by CERSAT. The second is from RSS who apply their own processing.

3.1.2.1. JPL/CERSAT (QS_CERSAT): This dataset comprises K_u-band microwave scatterometer data from the NASA SeaWinds scatterometer, onboard QuikSCAT (IFREMER/CERSAT, 2002b). Data have been processed up to level 2b (calibrated, geo-referenced swath winds) by the JPL (Dunbar *et al.*, 2006) and gridded fields constructed by CERSAT. The recommended vector wind ambiguities are used and wind vectors outside the range $0.5-30\,\mathrm{ms}^{-1}$ are excluded. The land mask is at 0.5° resolution. There are no wind values over polar sea-ice as determined from the scatterometer backscatter, the mask edge is at approximately the 40% sea-ice concentration limit.

Comparisons with *in situ* collocated winds (1 h and 25 km) from the National Data Buoy Center (NDBC), the Tropical Atmosphere Ocean (TAO) buoy array and European buoys converted to 10-m neutral winds using the method of Liu *et al.* (1979), showed an root mean square (RMS) error of less than $1.9\,\mathrm{ms}^{-1}$ and an overestimate by QuikSCAT relative to the buoys of about $0.35\,\mathrm{ms}^{-1}$ (IFREMER/CERSAT, 2002b). It is stated that QuikSCAT underestimates at low winds and overestimates at high winds (the opposite of the ERS scatterometers) but also that daily average values were overestimated at low wind speeds ($<4\,\mathrm{ms}^{-1}$; IFREMER/CERSAT, 2002b). RMS differences were smallest in the range $4-8\,\mathrm{ms}^{-1}$ and low wind speeds show larger RMS differences. As for ERS it is not clear from the documentation what combination of data quality flags have been used in the calculation of the monthly mean product. Winds are referenced to 10 m height at neutral stability.

3.1.2.2. RSS v4.0 (QS_RSS4): RSS published their version 4.0 data in April 2011. Data have been processed up to level 2a (backscatter, gridded swath data) by JPL (D. Smith, personal communication, 2011), version 4.0 level 2b (swath) and level 3 (gridded) $0.25^\circ \times 0.25^\circ$ fields are then produced by RSS at temporal resolutions of 12 h, 3 d, weekly and monthly, using their new model function Ku-2011 (Ricciardulli and Wentz, 2011). These wind speeds have been calibrated to rain-free WindSat data. Ricciardulli and Wentz (2011) present a comparison of QuikSCAT winds from Ku-2011 with buoy measurements that indicate agreement of $0.1 \pm 0.9\,\mathrm{ms}^{-1}$, although there is no information about which buoys were used or any adjustments applied to the buoy measurements.

RSS provide a rain flag along with their monthly mean wind files, however, the flag is only set when more than 20 (out of possible 60) observations were rain contaminated according to the rain flags provided with the 12-hourly wind product (D. Smith, personal communication, 2004). RSS recommend that for research purposes, daily files should be used to create monthly means according to the user's requirements concerning rain flags. For consistency with the CERSAT/JPL dataset we use RSS v4.0 as provided without the application of rain flags. Using the monthly rain flag as provided by RSS masks less than 1% of the data and has no effect on our findings. Winds are referenced to 10 m height at neutral stability.

3.1.3. Hamburg Ocean Atmosphere Parameters and Fluxes from Satellite Data Set version 3 (HOAPSv3; Andersson et al., 2007)

HOAPSv3 comprises data from the Special Sensor Microwave Imager (SSM/I). Intercalibration of brightness temperatures from different satellites is performed. Wind speeds are derived from brightness temperatures with a neural network (Andersson *et al.*, 2010). No information on direction is available. The neural network derives the 10-m wind speed directly from the brightness temperatures allowing for the nonlinear relationships involved and also for different atmospheric conditions such as clear sky or cloud. The network is trained using two datasets. The first is derived from radiosondes and contains simulated SSM/I brightness temperatures from the radiosonde profiles and near surface wind speeds. The second is collocated (within 30 min and 50 km) SSM/I brightness temperatures and buoy wind speeds from NDBC (20 buoys) and TAO (59 buoys). The buoy wind speed measurements were individually converted to a height of 10 m wind using a logarithmic wind profile assuming neutral stratification. The network is then trained using these two datasets combined, which is thought to ensure the representativeness of the input and output data from the neural network (Andersson *et al.*, 2010).

The mean fields are computed from the pixel-level data by averaging all SSM/I pixels that have their centre within the respective 0.5° grid box each month. The resulting data fields are multi-satellite averages and are supplemented by basic statistical information about standard deviation and number of observations per grid box. Winds are referenced to 10 m height at neutral stability (K. Fennig, personal communication, 2012). The HOAPS dataset has recently been updated to version 3.2 and contains data up to the end of 2008 (Fennig *et al.*, 2012).

3.1.4. National Oceanography Centre Surface Flux Dataset v2.0 (NOCv2.0; Berry and Kent, 2009, 2011)

NOCv2.0 is constructed from VOS *in situ* wind speed observations from version 2.4 of the International Comprehensive Ocean–atmosphere Data Set (ICOADS; Woodruff *et al.*, 1998; Worley *et al.*, 2005). From 2007 version 2.5 (Woodruff *et al.*, 2011) is used including real-time updates from 2008 onwards. Although ICOADS also contains observations from moored and drifting buoys these are excluded. Only observations within 4.5 standard deviations of the climatological monthly mean value, as determined from the ICOADS trimming flags, are used. Additionally, observations shown to be mislocated were excluded (Kent and Challenor, 2006).

ICOADS VOS wind speeds are either measured using an anemometer or visually estimated from the sea state and converted to a speed using a Beaufort equivalent scale (Kent and Taylor, 1997). The methods of measurement preferred by the VOS have changed over time, with the use of anemometers becoming more common (Thomas *et al.*, 2008), and the average measurement height has increased (Kent *et al.*, 2007). Visual wind estimates have been adjusted to account for biases in the Beaufort scale used to report the data (Kent and Taylor, 1997) following Lindau (1995). Anemometer wind speeds are adjusted to a standard level of 10 m above sea level using the wind profile relation of Smith (1980) and known measurement heights, where available (Kent *et al.*, 2007). Where heights were unknown, the defaults were based on a 2° area monthly gridded dataset of anemometer heights.

Comparisons of adjusted visual and anemometer winds confirmed the conclusion of Thomas *et al.* (2008) that additional adjustments are required to visual winds to improve agreement with adjusted anemometer winds (Berry and Kent, 2011). The additional adjustment was applied to individual visual wind speed estimates using a simple scaling factor. Prior to the end of 1985 the factor is 1, from the start of 2000 the factor is 0.95, and values in the intervening period are found by linear interpolation. Visual wind speeds dominated until the end of the 1970s and by 2004 had dropped to less than a third of observations (Thomas *et al.*, 2008). The residual bias uncertainty in the mean wind speed from each method was estimated to be $0.2\,\mathrm{ms}^{-1}$ (Berry and Kent, 2011). Wind speeds are referenced to 10 m height and are stability-dependent.

The optimal interpolation (OI) scheme used follows Reynolds and Smith (1994). OI is performed on the individual observations, relative to a first guess field, and normalized by the uncertainty in the first guess (Berry and Kent, 2011). A weekly ice mask, based on Reynolds *et al.* (2002), was used to exclude those regions covered by ice from the analysis. Daily wind speed fields were produced which were averaged to give a monthly mean. Daily uncertainties are produced from the OI scheme and were weighted by the expected correlations in the data to produce monthly estimates of the uncertainty (Berry and Kent, 2011).

3.1.5. National Centers for Environmental Prediction (NCEP)/National Center for Atmospheric Research (NCAR) Reanalysis version 1 (NCEP; Kalnay et al., 1996)

Wind speeds from the first-generation NCEP reanalysis are available from 1948 until the present. The analysis system was identical to the NCEP global operational model implemented in January 1995, except that it had a horizontal resolution of about 210 km. Fields are not expected to be of as high quality as a modern forecast model. However NCEP/NCAR1 has been widely studied, is available for the full satellite period and does not incorporate satellite winds from scatterometers or from SSM/I and is therefore independent of those datasets (Table 1). Wind speeds from NCEP are referenced to 10 m height and are stability-dependent.

Output parameters are classified according to their dependence on observations or on the model. Level A parameters are those which are strongly constrained by observations, and include the wind components at the model grid levels. Winds at 10 m are an output of the boundary layer scheme and are therefore more model dependent and hence classified as a level B parameter (Kalnay *et al.*, 1996).

3.1.6. Twentieth Century Reanalysis version 2 (C20Rv2; Compo et al., 2011)

C20Rv2 provides 6-hourly, daily and monthly fields on a 2° grid from 1871 to 2010. C20Rv2 is a global atmospheric circulation dataset, assimilating only surface pressure reports over both the land and ocean and using observed monthly SST and sea-ice as boundary conditions. It uses an Ensemble Kalman Filter data assimilation method with background first guess fields supplied by an ensemble of forecasts from a global numerical weather prediction model. This directly yields a global analysis every 6 h as the most likely state of the atmosphere, and also an uncertainty estimate of that analysis through the spread of the ensemble. The SST and sea-ice come from the HadISST dataset (Rayner *et al.*, 2003) and marine pressure observations come from ICOADS Release 2.4 (from 1952; Worley *et al.*, 2005) and ICOADS Release 2.5 (from 1871; Woodruff *et al.*, 2011). No wind observations are assimilated into C20Rv2. The fields are referenced to 10 m height and are stability-dependent.

3.1.7. European Centre for Medium-Range Weather Forecasts (ECMWF) Interim Reanalysis (ERAI; Dee et al., 2011)

ERAI covers the time period 1979 until the present, using a 12-h 4D-Var data assimilation system (Uppala *et al.*, 2008a, 2008b; Dee *et al.*, 2011). Presently data for the period 1979–2012 are publicly available from

the ECMWF data server at $0.75^\circ \times 0.75^\circ$ (Berrisford *et al.*, 2009). However this study uses data from 1989 to 2009 at $1.5^\circ \times 1.5^\circ$ as was available prior to May 2012. Uppala *et al.* (2008a, 2008b) describe the main advances of the ERAI data assimilation over the previous reanalysis (ERA40; Uppala *et al.*, 2005). ERAI relies mostly on observations prepared for ERA40 supplemented by data for later years from the ECMWF operational archive. Several different SST and sea-ice concentration datasets are used with changes in July 2001, January 2002 and February 2009 (Dee *et al.*, 2011). Some new or reprocessed datasets have been utilized including winds obtained from feature tracking of Meteosat images. Table 1 summarizes the input surface wind speed data. ERAI is available as monthly means of daily means of 10-m, stability-dependent, wind speed data.

Initial indications are that the interannual variability of ERAI winds is better than that in ERA40, which was already superior to other reanalysis wind products (Trenberth *et al.*, 2010). Surface wind speeds are also stronger than in ERA40 due to the improved model resolution.

3.1.8. Blended sea winds (BSW; Zhang et al., 2006a, 2006b)

The National Oceanic and Atmospheric Administration (NOAA) National Environmental Satellite, Data and Information Service (NESDIS) BSW product (Zhang *et al.*, 2006a, 2006b) contains globally gridded, high resolution ocean surface vector winds and wind stresses on a 0.25° grid, and multiple time resolutions of 6-hourly, daily, monthly and 11-year (1995–2005) climatological months. The period of record is 9 July 1987 – present. The wind speeds were generated by blending observations from multiple satellites: the Defense Meteorological Satellites Program (DMSP) SSM/I; the Tropical Rainfall Measuring Mission (TRMM) Microwave Imager (TMI); QuikSCAT and the Advanced Microwave Scanning Radiometer – Earth Observing System (AMSR-E). The wind directions are from NCEP/Department of Energy (DOE) Reanalysis 2 (Kanamitsu *et al.*, 2002), and are interpolated onto the blended speed grids. All satellite data are sourced from RSS and were the latest versions as of October 2005 as described by Zhang *et al.* (2006b). BSW does not make use of any C-band scatterometer data (e.g. ERS1, ERS2).

Interpolation is by a simple objective analysis method, namely a spatio-temporally weighted interpolation, which is used to generate a 12-hourly blended product from multiple satellites. Space-time aliases are addressed following Zeng and Levy (1995). Weighting is Gaussian within a window of 62.5 km and 6 h either side from the grid box centre. Daily and monthly data fields are obtained by averaging the 12-hourly values, 6-hourly data fields are interpolated from 12-hourly values. Before 1999 (i.e. prior to the launch of QuikSCAT), BSW data have systematic gaps at low latitudes caused by sparse sampling in these regions. These gaps are not filled by the interpolation technique. No account is taken of the expected quality of individual data sources or of potential biases between data sources. Ten-metre neutral equivalent wind speeds are provided.

3.1.9. Cross-calibrated multi-platform (CCMP; Atlas et al., 2011)

CCMP Ocean Surface Wind Components blended product from NASA combines data from several satellite and *in situ* sources using ERA40 (Uppala *et al.*, 2005) as a background field from 1987 to 1999 and ERA operational model output thereafter. *In situ* observations are obtained from NCAR and include ICOADS, further observations provided and quality controlled by NCEP (D. Moroni, personal communication, 2012) and additional observations from the TAO and PIRATA moored buoy arrays. Observations are adjusted to 10 m assuming neutral stability, where instrument heights are not available a default of 19.5 m is used for ship observations and 5 m for buoys. A variational analysis method (VAM) is used to combine wind measurements derived from SeaWinds on QuikSCAT, SeaWinds on ADEOS-II, AMSR-E, TRMM TMI and SSM/I for the period July 1987 to the present. All satellite data are obtained from RSS.

The VAM follows Atlas *et al.* (1996) and satisfies multiple constraints including minimizing the misfit of the analysis to the background field and the assimilated input data. The additional constraints include the magnitude of differences between analysis and background, that differences in speed, vorticity and divergence should be smooth and also that the rate of change of vorticity should be small. The VAM has been shown to be able to represent cyclones and storms that are missing or underrepresented in the background field (Atlas *et al.*, 2011). Improvements were required over the Atlas *et al.* (1996) scheme to allow for asynopticity. No information on the relative weighting of the different input data sources is given. Details of the cross-calibration of data sources are not currently available.

The VAM requires a prior estimate of the wind field. For the period July 1987 to December 1998, 10-m winds from ERA40 were used and from 1999 the ECMWF operational analysis (Atlas *et al.*, 2011). The winds provided are 10-m neutral wind speeds, although the background field is stability-dependent.

3.1.10. OAFlux (Yu and Weller, 2007)

The Woods Hole Oceanographic Institution (WHOI) OAFlux-blended product combines data from models and satellites according to weightings derived from comparisons with moored buoys deployed by WHOI (Yu and Weller, 2007). Wind data sources are the two NCEP Reanalyses, ERA40, SSM/I (version 6), AMSR-E (version 5) and QuikSCAT (version 3). All the satellite data were obtained from RSS. Daily 1° resolution fields are estimated using objective analysis from all data sources available at a particular time. Each of the reanalyses has a weight of 1, each satellite source a weight of 4 (Yu *et al.*, 2008). The objective analysis minimizes

differences between the solution and high quality buoy deployments. Solution is by a conjugate-gradient method used iteratively (Yu and O'Brien, 1991, 1995).

The variable estimates are sensitive to weights in regions where input data sources have large uncertainties and are less dependent on weights in regions where input datasets have good accuracy (Yu *et al.*, 2004). Error estimates are computed based on the assumptions that the errors from every input data source are uncorrelated with the errors from another input data source, and that, at a given location and a given day, the accuracy of the field estimate depends on the scatter among the input data (Yu *et al.*, 2008). The input datasets are a mixture of stability-dependent and neutral wind speeds. The output is a 10-m neutral equivalent wind speed (Yu *et al.*, 2008).

3.2. Data processing

For global datasets (ERAI, NCEP and C20Rv2), the appropriate land mask was used to generate an ocean-only dataset. The remainder of the datasets are ocean-only. Each dataset was then averaged to a 1° latitude–longitude grid referenced to the centre of each 1° range. Averages are calculated using cos(latitude) area weighting and any grid boxes on the original grid that fall partially within a grid box on the target grid are weighted appropriately.

Neutral values for ERAI and NOCv2.0 were calculated using stability-dependent bulk formulae at full resolution ($1.5^\circ \times 6$ h for ERAI and $1^\circ \times$ daily for NOCv2.0). There were small differences between the monthly mean wind speeds provided by ECMWF and the monthly average of the 6-hourly analysis values. We therefore used the average of the 6-hourly values for both the stability-dependent and neutral values for consistency. Any 6-hourly value where the corresponding fractional ice concentration was greater than zero was discarded, monthly grid box means were formed from any remaining 6-hourly values. Then any grid boxes with sampling of less than 75% over the ERAI period were also discarded.

4. Factors causing differences among datasets

4.1. Atmospheric stability

The importance of accounting for stability in comparisons between satellite and *in situ* winds has long been recognized (Askari *et al.*, 1993; Offiler, 1994; Colton *et al.*, 1995). This requires estimates of the stability of the surface atmospheric boundary layer that are not available from the satellite observations. It is therefore necessary to use information from a different source to make the required adjustment. Wallcraft *et al.* (2009) convert neutral winds from QuikSCAT to stability-dependent values using 6-hourly atmospheric variables from ERA40. However for SSM/I they adopt the simpler approach of assuming a constant offset of $0.2\,\mathrm{ms}^{-1}$. Wallcraft *et al.* (2009) justify this approach by referencing results comparing 10 years of SSM/I data with global analysis products published by Meissner *et al.* (2001). Meissner *et al.* (2001) however do not attribute the $0.2–0.3\,\mathrm{ms}^{-1}$ average low bias of the analyses to stability and no spatio-temporal characteristics of the offset are described. Chelton and Freilich (2005) also quote an adjustment of $0.2\,\mathrm{ms}^{-1}$ based on work published by Mears *et al.* (2001). However, Mears *et al.* (2001) found a mean difference between neutral stability and stability-dependent wind speeds of only $0.12\,\mathrm{ms}^{-1}$. Kara *et al.* (2008b) studied the effects of air–sea stability on wind speeds over the ocean and found a $0.2\,\mathrm{ms}^{-1}$ global mean offset between QuikSCAT and moored buoys. However, globally QuikSCAT data are increased by a smaller amount, an example of $0.07\,\mathrm{ms}^{-1}$ in July 2001 is quoted. Kara *et al.* (2008b) note that differences between neutral and stability-dependent wind speeds can be regionally important.

It is clear from the literature that neutral wind speeds are expected to be stronger, on average, than stability-dependent wind speeds. The size of the difference, of order $0.2\,\mathrm{ms}^{-1}$, is similar to the wind speed adequacy requirement for accurate surface fluxes. It is therefore necessary to account for the effects of stability before comparing satellite-derived wind speeds with those from *in situ* or model sources that are stability-dependent. Figure 1 shows the adjustment to neutral wind speed as calculated for ERAI using the COARE3.0 bulk formula (Fairall *et al.*, 2003). The adjustment varies regionally and seasonally. Figure 2 (solid line) shows the same information but averaged zonally and on average the largest adjustment is required in the Tropics where wind speed is low, but variability is higher in the Extratropics where day-to-day variations in the adjustments can be an order of magnitude larger than the mean value.

Uncertainties in the adjustment for stability due to the use of different bulk formulae (Kara *et al.*, 2008b) or in the input parameters required to make the adjustment (Chelton and Freilich, 2005) have led some to neglect the adjustment entirely (Chelton and Freilich, 2005) and others to apply a simple global offset (Wallcraft *et al.*, 2009). Figure 2 shows the zonal and annual average adjustment for stability calculated from different datasets and with different algorithms. There are noticeable differences between the adjustment calculated for ERAI using the COARE3.0 bulk formula and that for NOCv2.0 calculated using Smith (1980, 1988). However Figure 3 shows that the monthly mean adjustment from either dataset is larger than their differences. Figure 2 shows the zonal mean difference due to stability for ERAI using the Smith (1980, 1988) formulae and for NOCv2.0 using Smith (1980, 1988). In most latitudes, the stability adjustment is similar to that calculated using the COARE3.0 algorithm. However in northern mid- to high-latitudes the differences in adjustment between the algorithms are similar in magnitude to those between NOCv2.0 and ERAI. Figure 4 compares stability adjustments from actual to neutral winds from COARE3.0 and Smith (1980, 1988); the adjustments are negative under stable conditions and positive under unstable conditions. Figure 4 shows that the discrepancies between NOCv2.0 and ERAI are largely due to differences in the algorithms under

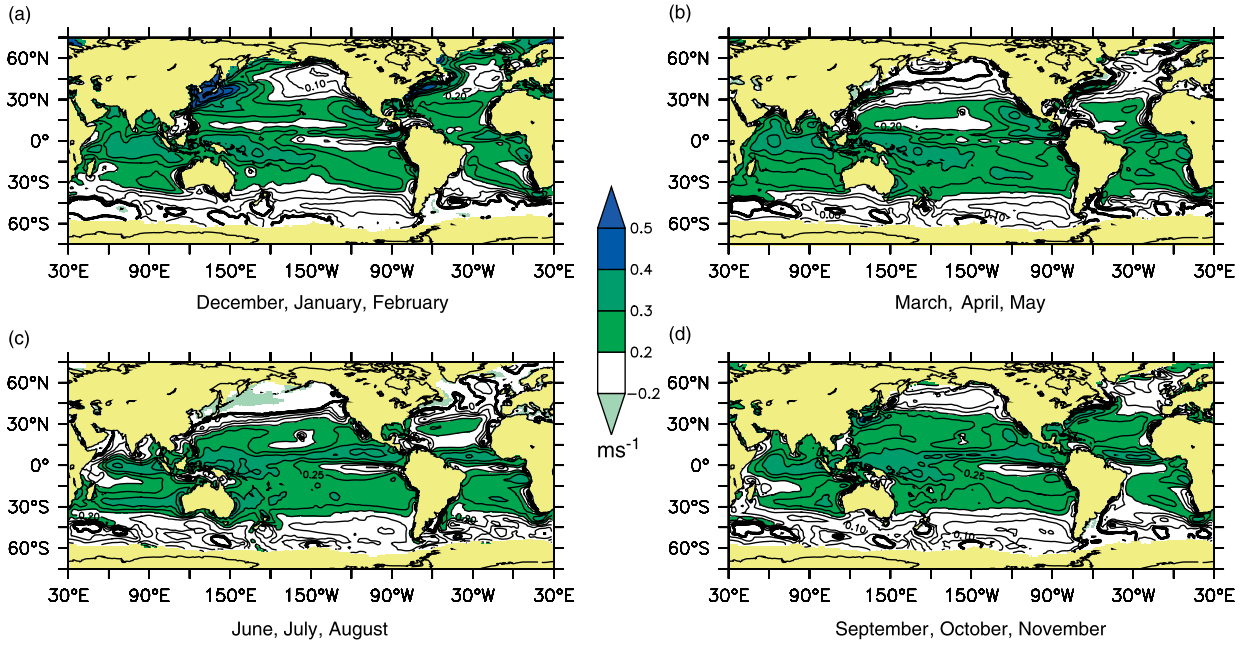

Figure 1. Seasonal average difference between 10 m neutral and 10 m stability-dependent winds (ms^{-1}) from ERAI 1989–2009, calculated using the COARE3.0 flux algorithm (Fairall *et al.*, 2003). The combined land and ice mask is shown in light grey (yellow online).

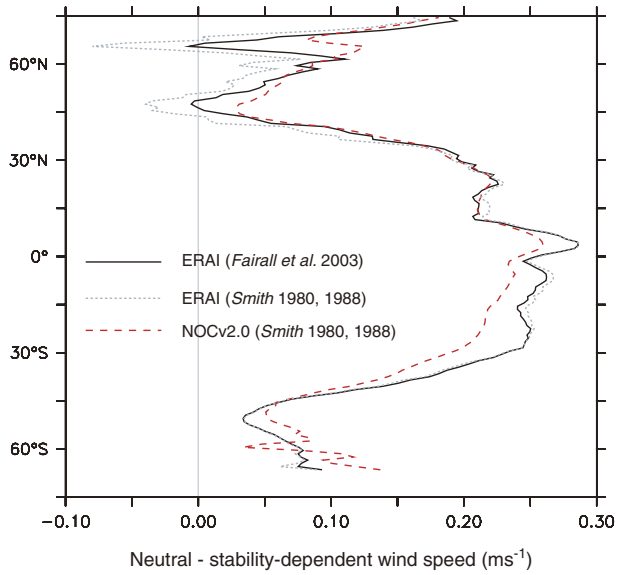

Figure 2. Annual average difference between 10 m neutral and 10 m stability-dependent winds (ms^{-1}). Solid line: ERAI 1989–2009 (as Figure 1); dashed line: NOCv2.0 1973–2009 using Smith (1980, 1988) flux algorithm (following Berry and Kent, 2009); dotted line: ERAI 1989–2009 but using Smith (1980, 1988) flux algorithm.

stable conditions. Under stable conditions COARE3.0 uses stability profiles following Beljaars and Holtslag (1991) whereas Smith (1980, 1988) follows Dyer (1974). Note that the ERAI uses the same stability profiles as COARE3.0 under stable conditions (ECMWF, 2007).

As a check on the stability adjustment we compare wind speeds from ERAI with those from CCMP. CCMP provides neutral values and Figure 5 shows that the agreement between the two datasets improves when ERAI is adjusted to neutral stability. The mean difference decreases from 0.16 ms^{-1} (CCMP higher than ERAI stability-dependent values) to 0.00 ms^{-1} when ERAI is adjusted for stability. The standard deviation of the monthly differences reduces slightly, from 0.64 to 0.60 ms^{-1}. Despite the improvements in the comparison there are still noticeable differences between the two datasets, both regionally, and over time (Figure 5).

Although there are differences between the adjustments for stability which depend on the algorithm used and the estimates of environmental parameters affecting the atmospheric stability, the differences are smaller than the typical magnitude of the adjustment itself. Adjusting wind speeds for datasets which provide stability-dependent values to neutral conditions improves the agreement among datasets. We therefore apply stability adjustments to the datasets providing stability-dependent wind speeds as described in Section 3.2. For NOCv2.0 we use the stability-dependent estimates following Smith (1980, 1988) as shown in Figure 2. For NCEP, C20Rv2 and ERAI we use the estimates calculated for ERAI using COARE3.0 (Fairall *et al.*, 2003) for the period 1989–2009.

4.2. Surface currents

Further differences between wind speed datasets are expected due to the effects of surface currents (Chelton *et al.*, 2004). Model-derived and *in situ* wind speeds are earth-relative, satellite and blended wind speeds are surface-relative. Blended datasets are thought to present surface-relative wind speeds but combine a mixture of surface-relative and earth-relative data sources. It is therefore expected that some of the differences between datasets might be explained in terms of the

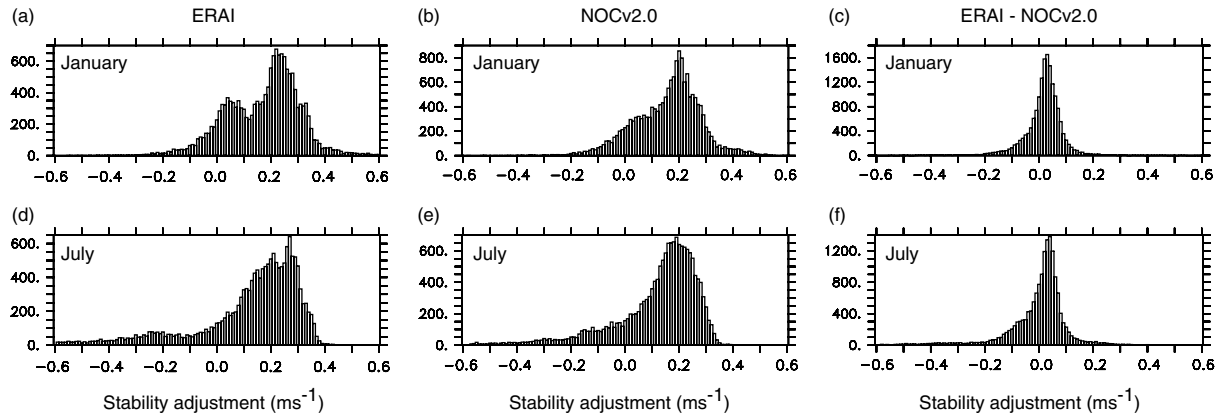

Figure 3. Histograms of climatological monthly difference between 10 m neutral and 10 m stability-dependent winds (ms^{-1}). NOCv2.0 values have been averaged onto to the ERAI spatial grid. Top row: January; lower: July. Left panel: stability adjustment from ERAI 1989–2009; centre panel: stability adjustment from NOCv2.0 1973–2009; right panel, difference in stability adjustment ERAI-NOCv2.0 1989–2009.

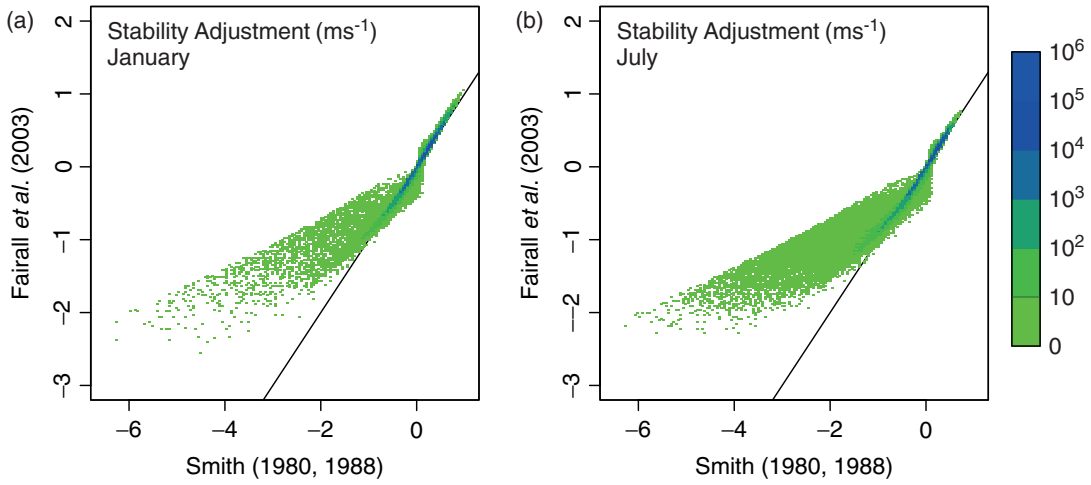

Figure 4. Density plot for the stability adjustment from stability-dependent to neutral equivalent wind speed calculated from ERAI analysis fields for (a) January and (b) July 2000 (ms^{-1}). The adjustment calculated using Smith (1980, 1988) following NOCv2.0 is plotted on the x-axis and that from COARE3.0 (Fairall *et al.*, 2003) on the y-axis. The black line indicates a 1 : 1 relationship.

surface currents. Atlas *et al.* (2011) compare CCMP and ECMWF operational analysis winds for a sample month following adjustment for stability. This reveals large-scale differences that can be attributed to currents and eddies and also potentially to persistent atmospheric or oceanic conditions affecting the microwave remote sensing of the ocean surface.

To quantify the expected difference between earth-relative and surface-relative wind speed estimates, surface current vectors collocated with every wind vector observation would be required. Although some estimates of surface currents are available (Bonjean and Lagerloef, 2002), we have not attempted to quantify the contribution of surface currents to the differences among the dataset. It should be noted that improved surface current estimates, probably at higher resolution, may in the future allow this source of difference to be accounted for.

4.3. Rain contamination of satellite measurements

Neither scatterometers nor passive microwave sensors can retrieve wind in the presence of rain and undetected rain can result in large biases in the measurements. Scatterometer measurements are affected more at K_u-band (e.g. QuikSCAT) than at C-band (e.g. ERS1 and ERS2). When there is rain the K_u-band backscatter is affected by the roughening of the sea surface by rain drops and also by scattering and absorption by rain drops in the atmosphere (Chelton and Freilich, 2005). Wallcraft *et al.* (2009) constructed a rain-free version of the QuikSCAT dataset. They conclude that rain contamination of QuikSCAT winds can result in an overestimation in excess of 1 ms^{-1} in Tropical regions, an overestimation of order 0.4 ms^{-1} in mid-latitudes and an underestimation of order 0.3 ms^{-1} in high-latitudes monthly means. The requirement to exclude K_u-band scatterometer wind vectors contaminated by rain is well-known (see Section 3.1.2). At C-band and low incidence angles $<30^{\circ}$, rain is generally considered transparent. However, although the effects of rain are small compared to K_u-band, some effect on the C-band signal exists (Melsheimer *et al.*, 2001; Contreras and Plant, 2006), mainly caused by the impinging of rain

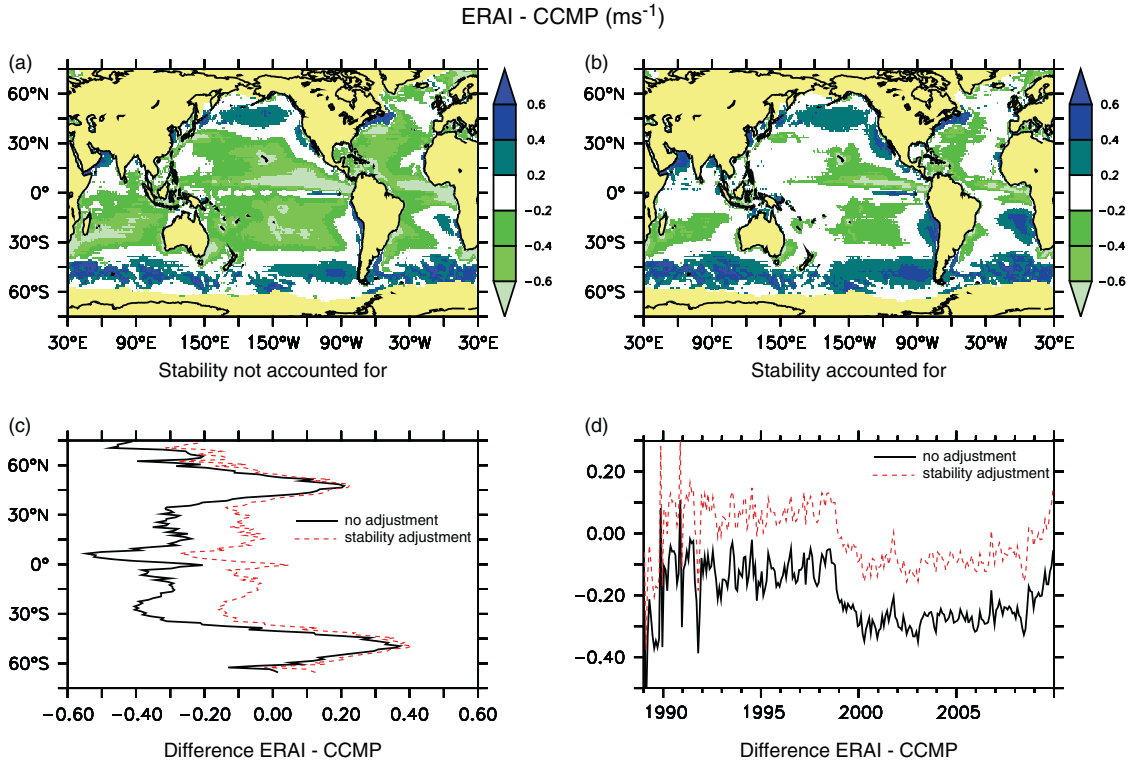

Figure 5. Difference ERAI minus CCMP (ms^{-1}) over their common period 1989–2009 showing the effect of stability adjustment (a) without stability adjustment; (b) ERAI adjusted for stability using COARE3.0; (c) zonal averages without stability adjustment (solid line) and with stability adjustment (dotted line); (d) as (c) but global monthly average values. The combined land and ice mask is shown in light grey (yellow online).

drops at the surface. The net effect on the radar backscatter is less well defined than at K_u-band and can result in an increase or a decrease of the signal (Melsheimer *et al.*, 2001). A small bias in the wind data cannot be ruled out. Passive microwave observations (e.g. SSM/I) are used to create rain flags for scatterometers because of their sensitivity to rain, however, there is currently no satellite mission combining both types of sensors and the temporal offset of scatterometer and passive microwave measurements can be problematic in this context.

Passive microwave observations can provide estimates of columnar rain rate but they cannot measure rain and wind simultaneously. Accordingly, passive microwave wind data can be expected to show a fair-weather bias due to under sampling of rainy conditions. Undetected rain is likely to result in an overestimate of wind speed from SSM/I but rain is relatively easy to detect so rain-affected observations are unlikely to significantly bias SSM/I wind speed datasets.

The analysis of biases due to unidentified rain contamination is complicated by expected relationships between wind speed and rain (see Section 4.4). An examination of the datasets suggests that the CCMP dataset has been fairly successful at removing rain contaminated wind observations from its analysis. Figure 6 shows the difference between wind speeds from QS_RSS4 and CCMP. Overlain are contours of precipitation from the Global

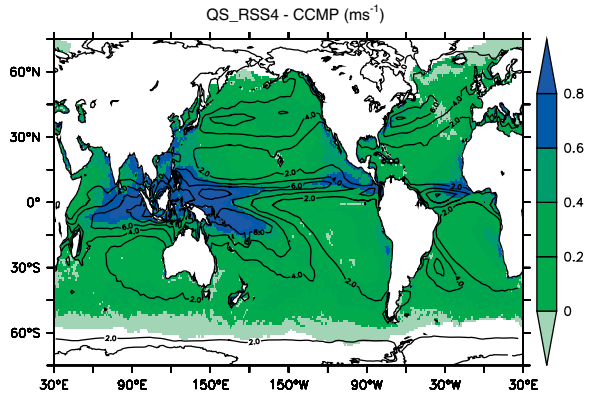

Figure 6. QS_RSS4 – CCMP wind speed difference (ms^{-1}) averaged over 1999–2009, colour bar. Line contours are precipitation from GPCP ($mm\,d^{-1}$).

Precipitation Climatology Project (GPCP; Adler *et al.*, 2003). The effect of rain is clear in the Tropics, with QS_RSS4 showing higher wind speeds than CCMP in regions of high precipitation as expected, but there are other differences between the datasets. Figure 6 suggests that we can use the characteristics of the differences of each data from CCMP to examine how the anomalies in each vary with rainfall amounts. In doing this we assume that CCMP shows no systematic rain contamination and realistically represents the relationship between mean wind and mean precipitation anomalies.

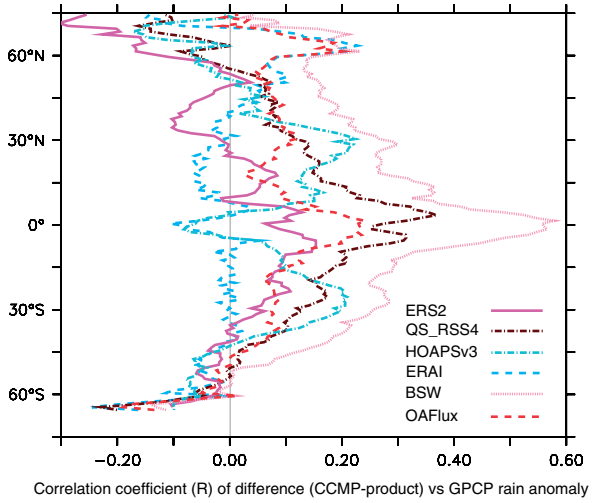

Figure 7. Zonal mean correlation of the monthly mean wind speed difference between CCMP and six other products and the monthly mean rain anomaly from GPCP.

We have used the correlations for the difference between wind anomalies from each dataset and from CCMP with rainfall anomalies from GPCP as an indicator of the effect of rain on each dataset (Figure 7). The correlations of BSW, QS_RSS4 and OAFlux differences from CCMP with rainfall anomalies all show a peak in the Tropics. The BSW dataset shows the largest correlations, which extend beyond the Tropics. These correlations exist prior to the launch of QuikSCAT (not shown) and so are not only due to the use of QuikSCAT in BSW. SSM/I data are used in BSW throughout the period and it seems likely that these data are responsible for the patterns of correlations seen. HOAPS reprocess the SSM/I data using their own neutral network algorithm and the result gives rather different patterns of correlation to BSW in both the pre-QuikSCAT and QuikSCAT periods (not shown). CCMP also ingests SSM/I data (from RSS; Atlas *et al.*, 2011) so it is clear that the methods of deriving wind speeds from the SSM/I data, screening and dataset construction have an important effect on the characteristics of the resulting wind speed fields.

ERAI assimilates QuikSCAT winds but does not show the same relationship with rain anomalies as the QS_RSS4 dataset. All of the datasets which do not incorporate QuikSCAT winds (ERS2 and HOAPS as shown in Figure 7, NCEP and C20Rv2, not shown) show a reduction in correlation at the equator (ERAI, HOAPSv3, C20Rv2 and NCEP show negative peaks in correlation) which may indicate some residual rain contamination in the CCMP dataset.

4.4. Fair-weather bias

The existence of a fair-weather bias in observations made by ships due to their potential avoidance of bad weather has long been suspected (Bunker, 1976) but never conclusively proved (Kent and Taylor, 1995; Gulev *et al.*, 2007). Satellite observations that are dependent on atmospheric conditions also have the potential for fair-weather bias (Andersson *et al.*, 2011). For example, the weather in the mid- to high-latitudes is dominated by atmospheric fronts with periods of high precipitation occurring with high wind speeds (Catto *et al.*, 2012). These effects will be screened out by the satellite data and may lead to a fair-weather bias in the satellite-based datasets. This impact has not been previously examined and to gain further understanding we have attempted to quantify the impact using *in situ* observations from ICOADS. VOS reports contain a weather code indicating whether or not there is precipitation at the time of the observation. This weather code has been used to generate datasets of all-weather wind speeds and of rain-free wind speeds. Figure 8 shows the difference between these datasets and hence an estimate of the potential fair-weather bias in any observing system that does not measure wind speed when it is raining. The mid-latitude storm tracks, and impact of the weather fronts, can be clearly seen with lower wind speeds under the no rain conditions compared to the all weather conditions (Figure 8(a)). These results suggest that the satellite wind speed estimates may be biased low by a few tenths ms^{-1} due to fair-weather bias in the mid-latitudes, the effect is larger in the winter than in summer (Figure 8(b)). The effect of fair-weather bias is smaller in the Tropics, although the effects of unidentified rain contaminated winds are likely to be large in the Tropics (Figure 6).

4.5. Coastal effects

Coastal winds are expected to be lighter than open ocean winds but stronger than the winds over land due to the orographic effect of the land (Kara *et al.*, 2008a). Hence, we would expect to see lighter winds in coastal regions compared to the open ocean. However, for datasets which combine or are representative of land and ocean data we would expect to see an enhanced effect in grid boxes containing both land and ocean due to contamination from the land data. Large mean differences between coastal and open ocean wind estimates are therefore likely to be an indication of coastal winds being representative of mixed land and oceanic conditions. This is a particular problem for low-resolution model-derived wind products with the winds typically underestimated in coastal regions (Kara *et al.*, 2008a). We expect a similar, but reduced, problem in OAFlux due to the inclusion of first and second NCEP reanalyses (Kalnay *et al.*, 1996; Kanamitsu *et al.*, 2002) and ERA40 (Uppala *et al.*, 2005).

Figure 9 shows the differences between QS_RSS4 and OAFlux wind speeds in two coastal regions. Largest differences are seen near almost all of the coasts, with OAFlux showing lower wind speeds than QS_RSS4. Figure 9 also shows similar patterns in a comparison of QS_RSS4 with ERAI (note that higher resolution fields from ERAI are now available but have not been used in this study). It seems evident that OAFlux wind speeds are biased low in coastal regions, and that this may be due to the inclusion of low-resolution wind speeds from atmospheric reanalyses.

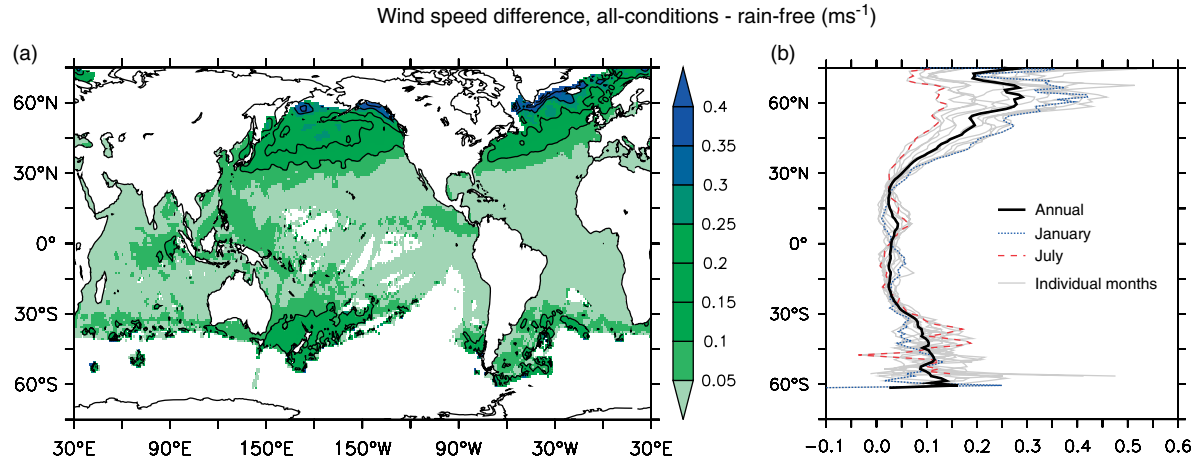

Figure 8. Difference between wind speeds for all conditions and rain-free conditions (ms^{-1}) estimated from ICOADS using methodology of Berry and Kent (2009, 2011). (a) Mean over 1970–2009, white regions are where insufficient data were available to form an estimate; (b) Zonal mean, annual and monthly.

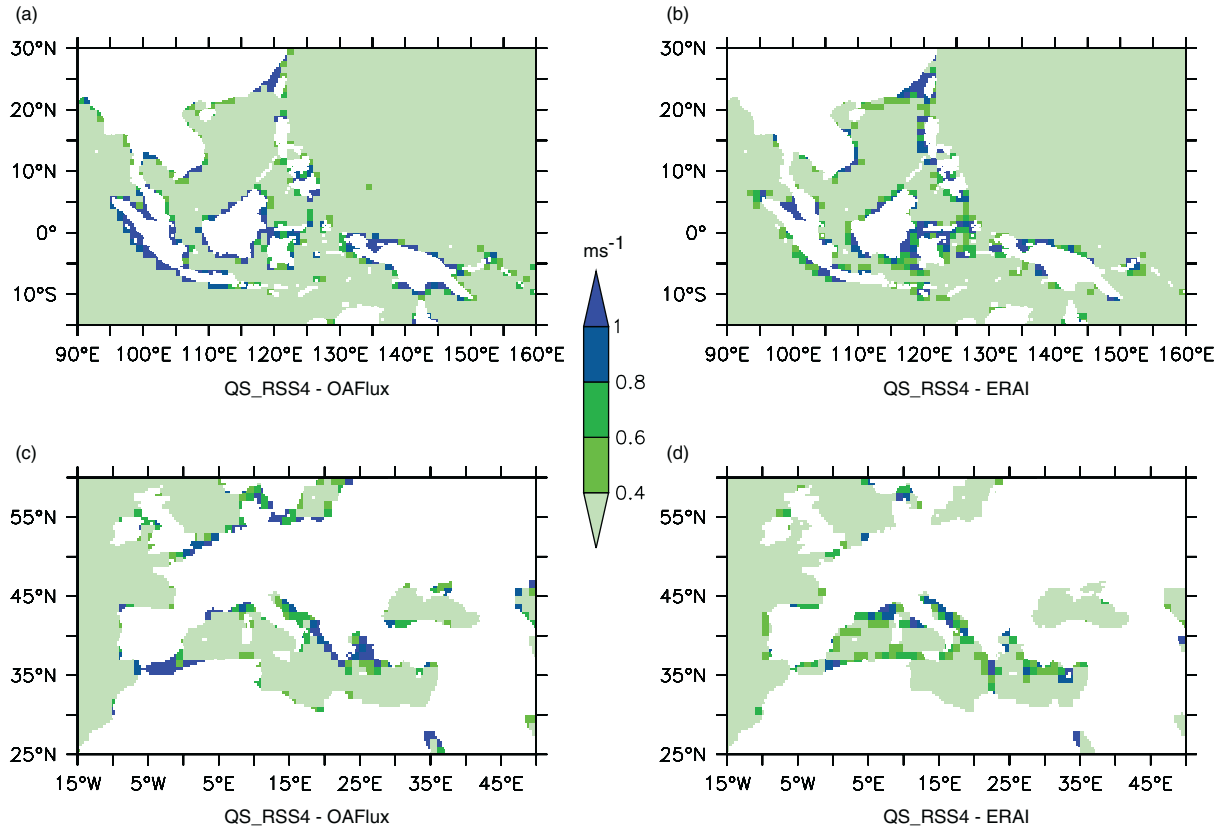

Figure 9. Difference between monthly mean wind speed products (ms^{-1}) over their common periods in two coastal regions: (a and b) Western Pacific/Indonesian region; (c and d) Europe/North Africa. In each case, the mean difference over the region has been removed. (a and c) QS_RSS4 – OAFlux; (b and d) QS_RSS4 – ERAI (adjusted to neutral conditions).

Figure 10 shows the difference between wind speeds averaged in coastal regions and in the open ocean. The characteristics of interest are (1) the mean differences and (2) whether or not the mean differences change with time. The lower-resolution model data, NCEP and ERAI, and the dataset that includes the model data, OAFlux, have the largest differences. The observation-based estimates have the smallest differences, with the two single source datasets, NOCv2 and QS_RSS4, being the smallest. Both NOCv2 and QS_RSS4 are based on purely marine data sources, from VOS and QuikSCAT respectively. The datasets that include data from different sources show an intermediate effect. The larger differences from the model-based datasets are expected due to the coastal boxes representing land and ocean conditions as described above. Similarly, OAFlux appears

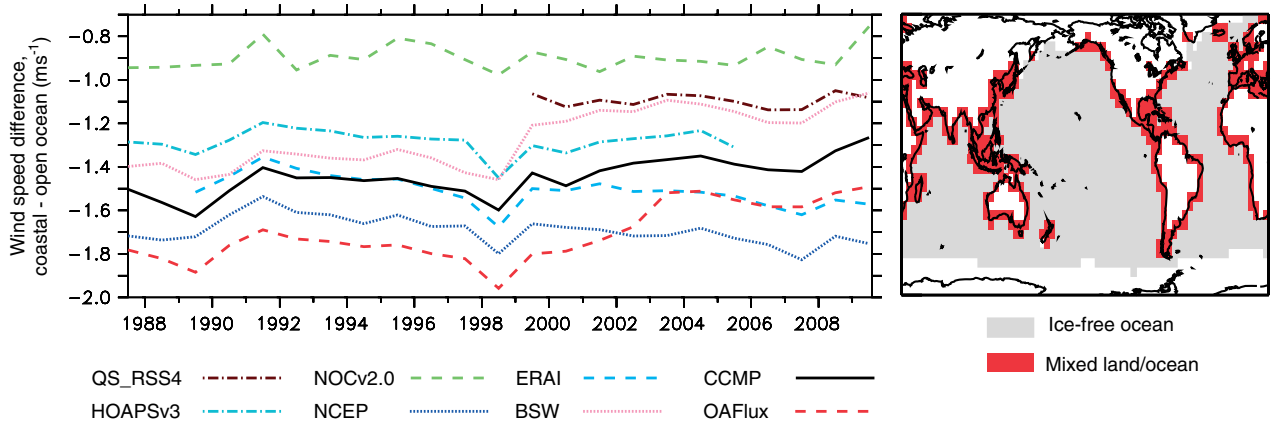

Figure 10. Left panel: Difference between annual mean wind speeds (ms^{-1}) in coastal and open ocean conditions, 1987–2009. Right panel: red indicates mixed land/ocean 1° grid boxes classed as coastal, the grey shading indicates ice-free regions classed as open ocean.

to suffer from this problem due to the inclusion of the model data. The QS_RSS4 data is expected to be the most representative of coastal conditions due to the higher resolution of the data and use of a single source. The smaller differences for NOCv2 might suggest that it is more representative of open ocean than coastal conditions.

The majority of the time series shown in Figure 10 exhibit little change over the period. The exceptions are those that include QuickSCAT data. There is a clear step in the BSW data coincident with the beginning of the QuickSCAT data and a similar, but smaller, step is evident in the CCMP data. The OAFlux data also shows a long-term change but this is more gradual due to changing sources of data used. The period of change includes the start of the QuickSCAT data, the loss of the ERA40 fields and the availability of passive microwave data from AMSR-E.

4.6. Monthly mean wind speeds

4.6.1. Spatial differences

Figure 11 shows maps of the differences of each dataset from CCMP over their common period. As in Section 4.3 CCMP was chosen because of its relatively good performance, for example, at excluding the effects of rain contamination. Differences for QS_CERSAT are similar to those from QS_RSS4 and are not shown. Neutral values are shown for NOCv2.0, NCEP, C20Rv2 and ERAI. The spatial patterns of differences vary substantially among the datasets. ERS1 (Figure 11(a)) and ERS2 (Figure 11(b)) show lower winds than CCMP in the Tropics and higher (ERS1) or similar (ERS2) wind speeds at higher latitudes. The differences for ERAI (Figure 11(h)) show some similarities to the ERS differences. QS_RSS4 differences (Figure 11(c)) show higher wind speeds in the Tropical rain bands (as also shown in Figure 6) and also some indication of higher wind speeds in the upwelling regions associated with the subtropical high pressure systems. HOAPS differences (Figure 11(d)) show higher wind speeds over much of the ocean, but similar or lower wind speeds in regions likely to have land influence (e.g. Arabian Sea, Bay of Bengal, and off the West Coasts of Australia and the major continents), (Andersson *et al.*, 2011). BSW differences (Figure 11(i)) show a combination of those seen in HOAPS and QS_RSS4. Differences for NOCv2.0 (Figure 11(e)) are noisy in regions outside the main shipping lanes but show higher wind speeds in the upwelling regions where QS_RSS4 also showed higher wind speeds [also shown by NCEP (Figure 11(f)), C20Rv2 (Figure 11(g)), ERAI and to a lesser extent in ERS1, ERS2 and OAFlux (Figure 11(j))]. This suggests that CCMP may be affected by low wind speeds from SSM/I in these regions, as also suggested by Atlas *et al.* (2011, Figure 10). SSM/I wind speeds are thought to be sensitive to some unaccounted for atmospheric or oceanic condition. Cold upwelling, stability, coastal fog and low-lying stratus are all suspect, but to date extensive RSS studies have yet to confirm or rule out these hypotheses (Atlas *et al.*, 2011).

Differences for NCEP (Figure 11(f)) and C20Rv2 (Figure 11(g)) are similar in pattern, with NCEP winds stronger than C20Rv2. The spectral signature of the C20Rv2 model is evident as oscillations in long-term mean values (G. P. Compo, personal communication, 2010). OAFlux (Figure 11(j)) is the most similar to CCMP but shows higher values in the regions where SSM/I is likely to be too low, but also in the Tropical rain band region where QuikSCAT measurements can be biased high by rain.

4.6.2. Time series

Figure 12 shows the average annual mean wind speed and mean seasonal cycle from each *in situ*, reanalysis and blended dataset for whole years for the Northern Extratropics (Figure 12(a)), the Tropics (Figure 12(b)); the Southern Extratropics (Figure 12(c)) and Global ice-free ocean (Figure 12(d)). Again neutral values are shown for NOCv2.0, NCEP, C20Rv2 and ERAI. NOCv2.0 contains large uncertainties in the Southern Extratropics, and hence in the global mean, and has been

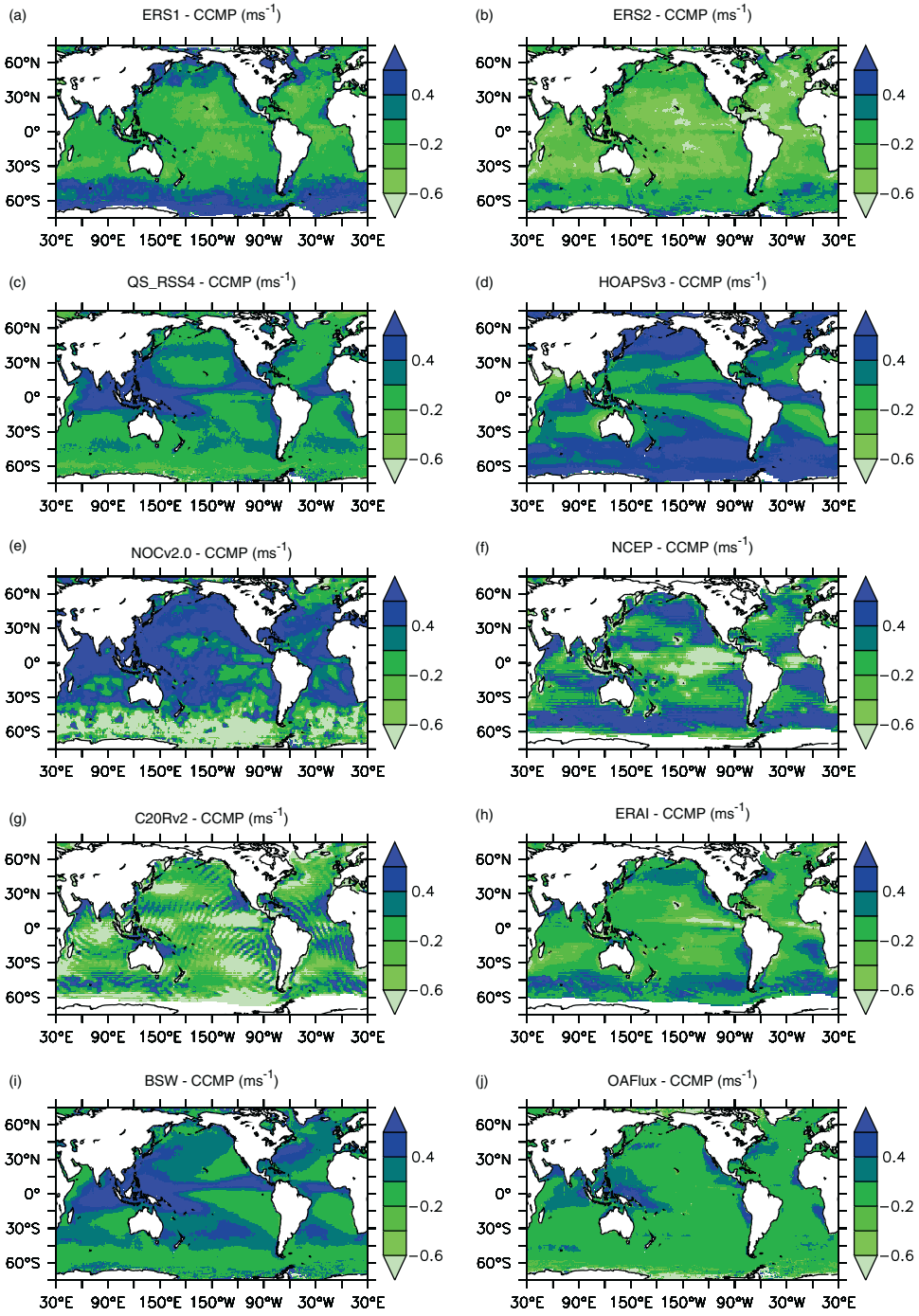

Figure 11. Differences from CCMP wind speed (ms^{-1}) averaged over the common period for each dataset (colour bar). Stability-dependent wind speeds have been converted to neutral stability: NOCv2.0 (Smith, 1980, 1988), ERAI (using Fairall *et al.*, 2003), NCEP (using ERAI adjustments) and C20Rv2 (using ERAI adjustments).

excluded from Figure 12(c) and 12(d). Figure 13 shows the same information for the satellite datasets. CCMP is plotted on both Figures 12 and 13 for comparison. There is a wide range of mean values at all latitudes. In the Northern Extratropics, there is nearly $1\,ms^{-1}$ between the highest (NOCv2.0) and lowest (C20Rv2) mean wind speeds. In the Northern Extratropics, the range of difference increases over time as most of the observational and blended datasets show an increase over the period 1989–2009 whereas the reanalyses (NCEP, C20Rv2 and ERAI) all show little change. In the Tropics most of the datasets show a slight increase in mean wind speed, NOCv2.0 shows a larger increase than the other datasets but fairly sparse sampling by ships means that uncertainty is relatively large for this dataset in the Tropics. In the Southern Extratropics, there is a smaller range of mean differences amongst the datasets, despite the poor sampling by *in situ* observations. Here, the reanalyses are less constrained by observations and ERAI shows little change over time. In the Northern and Tropical regions

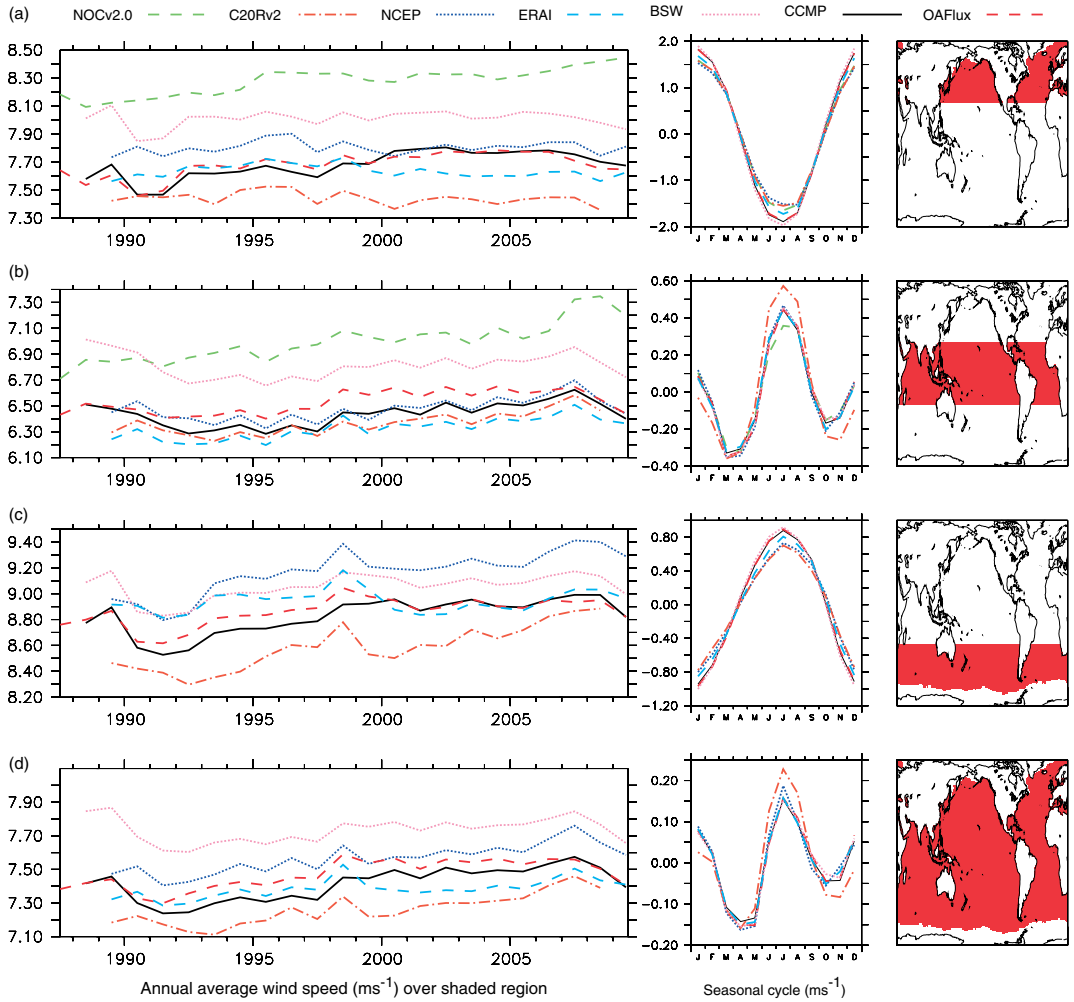

Figure 12. Annual mean wind speed and seasonal cycles (ms^{-1}) for *in situ*, renanalysis and blended datasets for the period 1987–2009. As in Figure 11, data from NOCv2.0, NCEP, C20Rv2 and ERAI have been converted to neutral values. Annual mean (left panels); seasonal cycle relative to annual mean (centre panels); mask showing data averaged (right panels). (a) 25°N–75°N; (b) 25°S–25°N; (c) 75°S–25°S; (d) 75°S–75°N.

ERAI shows amongst the lightest mean winds, but in the Southern Extratropics ERAI winds are relatively strong at the start of the period and become more similar to, for example, CCMP by the end of the period. This may suggest that ERAI model errors tend to make southern hemisphere winds relatively strong and this effect is corrected by the assimilation of observations later in the period (see also Figure 5(d)). Andersson *et al.* (2011) also show a divergence of global monthly means from ERAI compared with those from HOAPSv3 and NOCv2.0. Linear trends for this relatively short period show very little consistency among the datasets (not shown).

One striking feature in Figure 13 is the offset of nearly $0.6\,ms^{-1}$ between the wind speeds from the ERS scatterometers and QuikSCAT during their full year of overlap in 2000 (Table 1), seen also by Lee and McPhaden (2008). Various authors have concluded that wind speeds from QuikSCAT are higher than winds from other sources: by $0.11\,ms^{-1}$ compared with adjusted winds from open-ocean NDBC buoys (Chelton and Freilich, 2005); by $0.4\,ms^{-1}$ compared with ERS2 (Bentamy *et al.*, 2000); by $0.9\,ms^{-1}$ in the North-East Atlantic and by $1.1\,ms^{-1}$ in the Mediterranean compared with ERS2 (Queffeulou *et al.*, 2003). Also, ERS data have been described as biased $0.5\,ms^{-1}$ low in a comparison with buoy wind speeds (Verhoef and Stoffelen, 2011). ERS1 shows stronger winds than ERS2 whereas most of the datasets show an increase over time. This is unexpected as the two instruments and the orbits are the same and Lee and McPhaden (2008) found the wind speeds from ERS1 and ERS2 to be similar. Further examination of the 2 month overlap period in 2006 (not shown in Figure 13 due to use of whole years only) would be necessary to exclude the possibility of a change in wind climate being responsible. QuikSCAT winds from CERSAT start off higher than QS_RSS4 but the difference decreases over time and in the Tropics the QS_CERSAT mean winds are lower than those from QS_RSS4 by the end of the QuikSCAT mission.

Mean wind speeds from the datasets that include SSM/I show relatively low values in the early 1990s, particularly in the Extratropics. This may be an effect of biases early

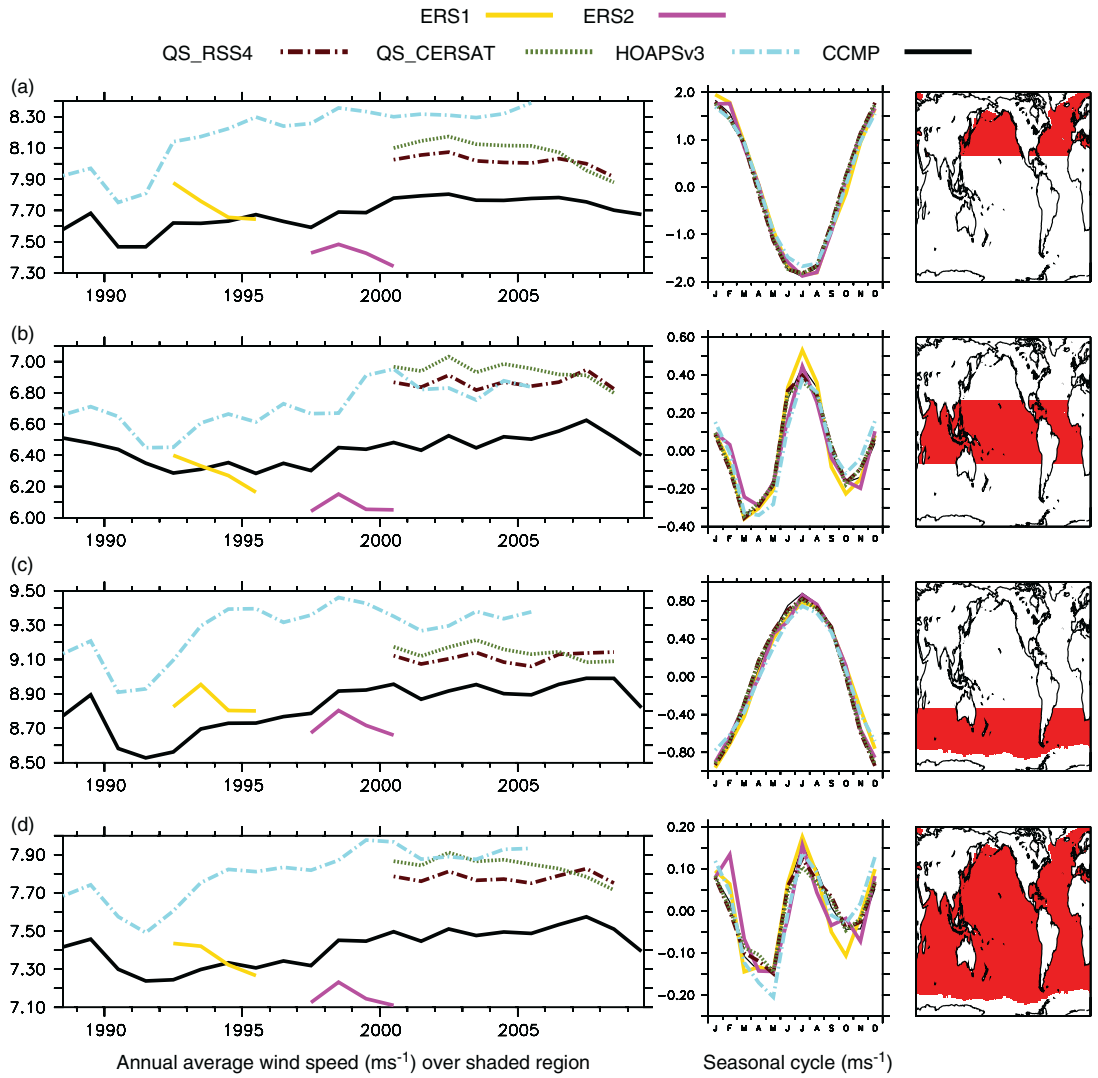

Figure 13. As Figure 12 but for satellite datasets. CCMP is also plotted to aid reference to Figure 12.

in the SSM/I observational period. This dip in mean wind speed is seen in CCMP, OAFlux, BSW (Figure 12) and HOAPS (Figure 13). These low wind speeds are not seen in the *in situ*, or scatterometer datasets nor in ERAI. NCEP does however show low wind speeds at this time in the Southern Extratropics (Figure 12(c))

In the Northern and Southern Extratropics, the blended datasets (BSW, CCMP and OAFlux) show larger seasonal cycles than the other datasets (Figure 12(a) and (c)). In the Tropics, C20Rv2 shows the strongest seasonal cycle (Figure 12(b)) which is probably unrealistic as C20Rv2 will not be well constrained by Tropical pressure observations. The other datasets show similar seasonal cycles except NOCv2.0 which probably underestimates the seasonal cycle due to its relatively large uncertainty in this region (Figures 12 and 13).

In the zonal mean (Figure 14), there is a range of order 1 ms^{-1} at most latitudes in the zonal mean wind estimates from the different datasets. QS_RSS4 shows relatively high wind speeds in the Tropical zonal mean (Figure 14(a) and (b)) but the standard deviation of the monthly means in the Tropics is the lowest of all the datasets (Figure 14(c)). HOAPS zonal mean wind speed is relatively high at most latitudes, but particularly in the Extratropics where the standard deviation is relatively low. NOCv2.0 zonal mean wind speeds are relatively strong in the Tropics and Northern Extratropics but poor sampling leads to winds that are too weak in the Southern Extratropics with a very high standard deviation showing poor representation of variability. NCEP and C20Rv2 winds show similar features with C20Rv2 agreeing better with CCMP than NCEP. Both datasets show relatively strong zonal mean winds in the Tropics with a high standard deviation. ERAI and the blended datasets (BSW, CCMP and OAFlux) all show similar features in the zonal mean.

5. Summary and conclusions

Although a variety of sources of wind speed data is available, none shows characteristics which would enable heat fluxes to be calculated to the target accuracy

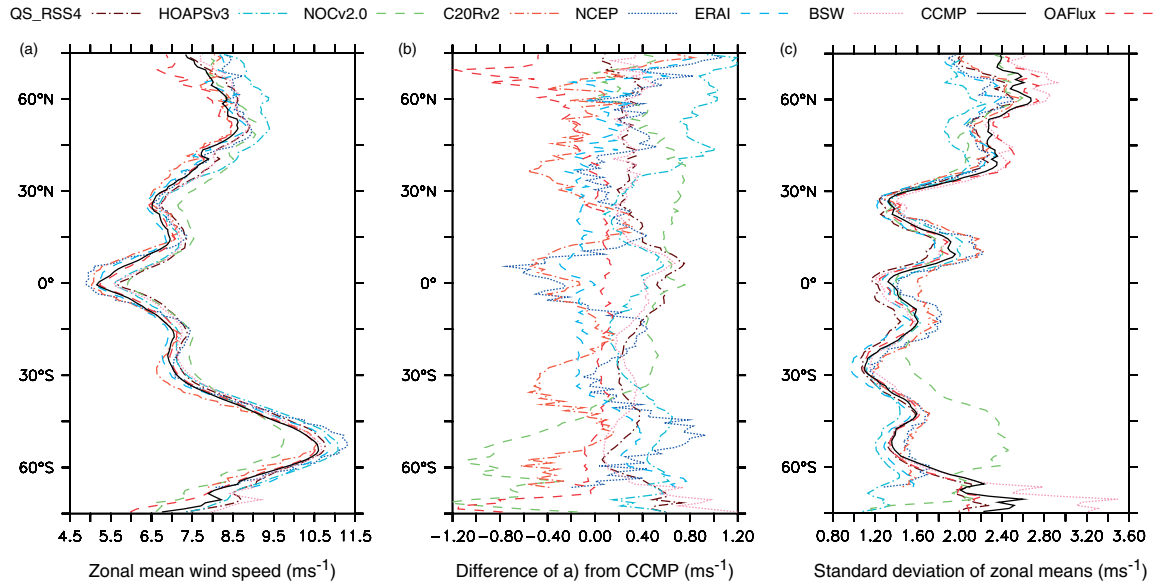

Figure 14. Zonal wind speeds (ms^{-1}). As in Figure 11, NOCv2.0, NCEP, C20Rv2 and ERAI have been converted to neutral stability. (a) Zonal mean wind speed; (b) as (a) but difference from CCMP; (c) standard deviation of monthly data as plotted in (a).

of 10 $W\,m^{-2}$ in the net heat flux. Comparison of wind speed data from different sources is complicated by the known effects of stability and surface currents. Satellite-derived wind speed data and products are presented as 10 m neutral equivalent wind speeds, and are surface-relative. *In situ* and model-derived data are typically 10 m stability-dependent wind speeds and are earth-relative. Neutral equivalent wind speeds can be calculated for many *in situ* datasets (e.g. from ships or moored buoys). Neutral equivalent winds can also be calculated from reanalyses, but any such calculation should be performed at the highest resolution possible and ideally be provided by the reanalysis centres in addition to the stability-dependent values. The information to calculate stability-dependent winds from satellite data is not typically available. Comparisons of surface stress, where available, would avoid this problem, however stress values calculated from stability-dependent wind speeds will be dependent on the form taken for the drag coefficient that may differ among the datasets being compared. Surface currents are more problematic as high-resolution global surface current vectors are not available. Most of the difference seen between, for example, ERAI and CCMP are accounted for by these known effects. Significant differences however remain.

The potential for contamination of scatterometer returns by rain is a significant, and well-known, problem. Differences of QuikSCAT datasets (QS_RSS4 and QS_CERSAT) from CCMP show correlations with rain anomalies that are also present, although smaller, in some blended datasets (e.g. BSW and OAFlux). Interestingly, the largest correlation is seen in the BSW dataset rather than either of the QuikSCAT datasets. This suggests that some of this correlation is coming from SSM/I data rather than QuikSCAT. SSM/I winds are expected to be biased high in the presence of rain, but rain is straightforward to detect and remove. HOAPS is based on SSM/I data and shows relatively low winds in regions where QuikSCAT is biased high by rain suggesting that unflagged rain is not the problem. Atlas *et al.* (2011) note that SSM/I is sensitive to certain atmospheric or oceanic conditions that have yet to be identified and it may be that these sensitivities are causing a positive correlation with anomalous rainfall. This conclusion is tentative as both CCMP and BSW ingest SSM/I winds from RSS.

Once rain contaminated data are successfully removed, the problem of fair-weather bias remains. This study has attempted to quantify the potential effects of fair-weather bias which suggests that effects are of the order a few tenths ms^{-1} in the seasonal mean, with maximum values in mid-latitudes in the winter months.

Coastal contamination of marine winds from global models has been noted before due to the transition from typically lower wind speeds over land to higher wind speeds over the ocean (Kara *et al.*, 2008a). We here show that wind speeds from ERAI in coastal regions are lower than those from datasets that use only marine data, for example, QuikSCAT and NOCv2.0. This underestimation of coastal wind speeds is also seen in OAFlux that blends model winds with marine-only satellite wind speeds.

Wind speeds from QuikSCAT are higher than those from the ERS scatterometers. The global mean difference is greater than 0.6 ms^{-1} (Verhoef and Stoffelen, 2011). There is a strong regional dependence in the differences, which may be partly due to rain contamination of QuikSCAT leading to an overestimation by over 1 ms^{-1} in Tropical regions. Another reason for the offset between the scatterometers may be the better sensitivity of QuikSCAT to higher wind speeds. However, the potential effects of contamination by precipitation or sea-ice mean that no firm conclusions can be drawn.

Taken together Figures 11 to 14 show that there is significant uncertainty in monthly winds, in mean values, spatial patterns and in changes over time. Some of the differences among the datasets can be attributed to known factors such as: rain effects on K_u-band scatterometer and SSM/I observations; problems with SSM/I retrievals in some atmospheric conditions and temporally variable observational constraints on reanalysis datasets. However, even for datasets that include the same source observations there remains structural uncertainty (Fangohr and Kent, 2012). This structural uncertainty increases when observations from different sources are combined using a variety of different methods.

The results of the comparisons of monthly mean wind speed datasets suggest that none of the sources of wind data presently available may meet the adequacy requirements for heat flux calculation of order $0.2\,\mathrm{ms}^{-1}$ in the monthly mean. The best candidate is the CCMP dataset, but questions remain about its accuracy in high-latitudes, the effect of fair-weather bias, the impact of biases in SSM/I observations and a possibility of residual rain contamination from QuikSCAT data in the Tropics. This needs to be explored further, using also *in situ* data where available which may require the construction of datasets withholding selected observations (Atlas *et al.*, 1996).

Acknowledgements

The International Comprehensive Ocean-Atmosphere Data Set (ICOADS) archive of surface marine observations underpins many of the datasets used in this study. Scott Woodruff, Sandy Lubker, Steven Worley and Eric Freeman have all provided help and expert advice on ICOADS when needed. ERS1, ERS2 and QuikSCAT (QS_CERSAT) monthly mean scatterometer data were obtained from CERSAT (http://www.ifremer.fr/cersat/en/data/gridded.htm). QuikSCAT data (QS_RSS4) are produced by Remote Sensing Systems (http://www.remss.com) and sponsored by the NASA Ocean Vector Winds Science Team. HOAPSv3 data were obtained from the World Data Center for Climate, Hamburg (http://www.hoaps.zmaw.de/). We are grateful to the National Center for Atmospheric Research for making the NOCv2.0 data available from the Computational and Information Systems Laboratory Research Data Archive (http://rda.ucar.edu/datasets/ds260.3/). NCEP Reanalysis data were provided by the NOAA/OAR/ESRL PSD, Boulder, Colorado, USA, from their Web site (http://www.esrl.noaa.gov/psd/). 20th Century Reanalysis V2 data were obtained from the NOAA/OAR/ESRL PSD, Boulder, Colorado, USA, (http://www.esrl.noaa.gov/psd/). Support for the Twentieth Century Reanalysis Project dataset is provided by the U.S. Department of Energy, Office of Science Innovative and Novel Computational Impact on Theory and Experiment (DOE INCITE) program, and Office of Biological and Environmental Research (BER), and by the National Oceanic and Atmospheric Administration Climate Program Office. ERA Interim data were downloaded from the ECMWF data server. Blended sea winds data were obtained from NOAA (http://www.ncdc.noaa.gov/oa/rsad/blendedseawinds.html). Cross-Calibrated Multi Platform data were downloaded from the JPL PO.DAAC site (http://podaac.jpl.nasa.gov/DATA_CATALOG/ccmpinfo.html). OAFlux data were provided by the WHOI OAFlux project (http://oaflux.whoi.edu) funded by the NOAA Climate Observations and Monitoring (COM) program. We are grateful to the anonymous reviewers whose careful and thoughtful comments have helped us to improve this paper.

References

Adler RF, Huffman GJ, Chang A, Ferraro R, Xie P, Janowiak J, Rudolf B, Schneider U, Curtis S, Bolvin D, Gruber A, Susskind J, Arkin P. 2003. The Version 2 Global Precipitation Climatology Project (GPCP) monthly precipitation analysis (1979-present). *Journal of Hydrometeorology* **4**: 1147–1167, DOI: 10.1175/1525-7541(2003)004<1147:TVGPCP>2.0.CO;2.

Andersson A, Bakan S, Fennig K, Grassl H, Klepp C-P, Schulz J, 2007. Hamburg Ocean Atmosphere Parameters and Fluxes from Satellite Data – HOAPS-3 – monthly mean. Electronic publication, World Data Center for Climate, DOI: 10.1594/WDCC/HOAPS3_MONTHLY.

Andersson A, Fennig K, Klepp C-P, Bakan S, Graßl H, Schulz J. 2010. The Hamburg ocean atmosphere parameters and fluxes from satellite data – HOAPS-3. *Earth System Science Data* **2**: 215–234, DOI: 10.5194/essd-2-215-2010.

Andersson A, Klepp C-P, Fennig K, Bakan S, Grassl H, Schulz J. 2011. Evaluation of HOAPS-3 ocean surface freshwater flux components. *Journal of Applied Meteorology and Climatology* **50**: 379–398, DOI: 10.1175/2010JAMC2341.1.

Askari F, Geernaert GL, Keller WC, Raman S. 1993. Radar imaging of thermal fronts. *International Journal of Remote Sensing* **14**: 275–294, DOI: 10.1080/01431169308904337.

Atlas R, Hoffman RN, Bloom SC, Jusem JC, Ardizzone J. 1996. A multiyear global surface wind velocity dataset using SSM/I wind observations. *Bulletin of the American Meteorological Society* **77**: 869–882, DOI: 10.1175/1520-0477(1996)077<0869:AMGSWV>2.0.CO;2.

Atlas R, Hoffman RN, Ardizzone J, Leidner SM, Jusem JC, Smith DK, Gombos D. 2011. A cross-calibrated, multiplatform ocean surface wind velocity product for meteorological and oceanographic applications. *Bulletin of the American Meteorological Society* **92**: 157–174, DOI: 10.1175/2010BAMS2946.1.

Beljaars ACM, Holtslag AAM. 1991. Flux parameterisation over land surfaces for atmospheric models. *Journal of Applied Meteorology* **30**: 327–341, DOI: 10.1175/1520-0450(1991)030<0327:FPOLSF>2.0.CO;2.

Bentamy A, Autret E, Queffeulou P, Quilfen Y, 2000. Intercomparison of ERS-2 and QuikSCAT Winds. *Geoscience and Remote Sensing Symposium, 2000. Proceedings. IGARSS 2000. IEEE 2000 International*, Vol.1, 234–236, DOI: 10.1109/IGARSS.2000.860477.

Berrisford P, Dee D, Fielding K, Fuentes M, Kållberg P, Kobayashi S, Uppala S, 2009. The ERA-Interim archive. *ERA Report Series*, No. 1, ECMWF, 20 pp.

Berry DI, 2009. Surface forcing of the North Atlantic: accuracy and variability. University of Southampton, School of Ocean and Earth Science, Doctoral Thesis, 176 pp.

Berry DI, Kent EC. 2009. A new air-sea interaction gridded dataset from ICOADS with uncertainty estimates. *Bulletin of the American Meteorological Society* **90**: 645–656, DOI: 10.1175/2008BAMS2639.1.

Berry DI, Kent EC. 2011. Air-sea fluxes from ICOADS: the construction of a new gridded dataset with uncertainty estimates. *International Journal of Climatology* **31**: 987–1001, DOI: 10.1002/joc.2059.

Bonjean F, Lagerloef GSE. 2002. Diagnostic model and analysis of the surface currents in the tropical pacific ocean. *Journal of Physical Oceanography* **32**: 2938–2954, DOI: 10.1175/1520-0485(2002)032<2938:DMAAOT>2.0.CO;2.

Bourassa MA, Vincent DG, Wood WL. 1999. A flux parameterization including the effects of capillary waves and sea state. *Journal of the Atmospheric Sciences* **56**: 1123–1139, DOI: 10.1175/1520-0469(1999)056<1123:AFPITE>2.0.CO;2.

Bourassa MA, Gille ST, Jackson DL, Roberts JB, Wick GA. 2010. Ocean winds and turbulent air-sea fluxes inferred from remote sensing. *Oceanography* **23**: 36–51, DOI: 10.5670/oceanog.2010.04.

Bourlès B, Lumpkin R, McPhaden MJ, Hernandez F, Nobre P, Campos E, Yu L, Planton S, Busalacchi AJ, Moura AD, Servain J, Trotte J. 2008. The PIRATA program: history, accomplishments, and future directions. *Bulletin of the American Meteorological Society* **89**: 1111–1125, DOI: 10.1175/2008BAMS2462.1.

Bradley EF, Fairall CW, 2007. A Guide to Making Climate Quality Meteorological and Flux Measurements at Sea. NOAA Technical Memorandum OAR PSD-311, NOAA/ESRL/PSD, Boulder, CO, 108.

Brunke MA, Fairall CW, Zeng X, Eymard L, Curry JA. 2003. Which bulk aerodynamic algorithms are least problematic in computing ocean surface turbulent fluxes? *Journal of Climate* **16**: 619–635, DOI: 10.1175/1520-0442(2003)016<0619:WBAAAL>2.0.CO;2.

Bunker AF. 1976. Computations of surface energy flux and annual air–sea interaction cycles of the North Atlantic Ocean. *Monthly Weather Review* **104**: 1122–1140, DOI: 10.1175/1520-0493(1976)104<1122:COSEFA>2.0.CO;2.

Catto JL, Jakob C, Berry G, Nicholls N. 2012. Relating global precipitation to atmospheric fronts. *Geophysical Research Letters* **39**: L10805, DOI: 10.1029/2012GL051736.

Chelton DB, Freilich MH. 2005. Scatterometer-based assessment of 10-m wind analyses from the Operational ECMWF and NCEP Numerical Weather Prediction Models. *Monthly Weather Review* **133**: 409–429, DOI: 10.1175/MWR-2861.1.

Chelton DB, Schlax MG, Freilich MH, Milliff R. 2004. Satellite measurements reveal persistent small-scale features in ocean winds. *Science* **303**: 978–983, DOI: 10.1126/science.1091901.

Clayson CA, Fairall CW, Curry JA. 1996. Evaluation of turbulent fluxes at the ocean surface using surface renewal theory. *Journal of Geophysical Research* **101**: 28503–28513, DOI: 10.1029/96JC02023.

Colton MC, Plant WJ, Keller WC, Geernaert GL. 1995. Tower-based measurements of normalised radar cross section from Lake Ontario: evidence of wind stress dependence. *Journal of Geophysical Research* **100**(C5): 8791–8813, DOI: 10.1029/95JC00364.

Compo GP, Whitaker JS, Sardeshmukh PD, Matsui N, Allan RJ, Yin X, Gleason BE, Vose RS, Rutledge G, Bessemoulin P, Brönnimann S, Brunet M, Crouthamel RI, Grant AN, Groisman PY, Jones PD, Kruk MC, Kruger AC, Marshall GJ, Maugeri M, Mok HY, Nordli Ø, Ross TF, Trigo RM, Wang XL, Woodruff SD, Worley SJ. 2011. The twentieth century reanalysis project. *Quarterly Journal of the Royal Meteorological Society* **137**: 1–28, DOI: 10.1002/qj.776.

Contreras RF, Plant WJ. 2006. Surface effect of rain on microwave backscatter from the ocean: measurements and modelling. *Journal of Geophysical Research* **111**(C8): C08019, DOI: 10.1029/2005JC003356.

Dee DP, Uppala SM, Simmons AJ, Berrisford P, Poli P, Kobayashi S, Andrae U, Balmaseda MA, Balsamo G, Bauer P, Bechtold P, Beljaars ACM, van de Berg L, Bidlot J, Bormann N, Delsol C, Dragani R, Fuentes M, Geer AJ, Haimberger L, Healy SB, Hersbach H, Hólm EV, Isaksen L, Kållberg P, Köhler M, Matricardi M, McNally AP, Monge-Sanz BM, Morcrette J-J, Park B-K, Peubey C, de Rosnay P, Tavolato C, Thépaut J-N, Vitart F. 2011. The ERA-Interim reanalysis: configuration and performance of the data assimilation system. *Quarterly Journal of the Royal Meteorological Society* **137**: 553–597, DOI: 10.1002/qj.828.

Dunbar RS, Lungu T, Weiss B, Stiles B, Huddleston J, Callahan PS, Shirtliffe G, Perry KL, Hsu C, Mears C, Wentz F, Smith D, 2006. QuikSCAT Science Data Product User Manual, Version 3.0, JPL Document D-18053 – Rev A, Jet Propulsion Laboratory, Pasadena, CA. Retrieved October 17, 2012. Available at http://dss.ucar.edu/datasets/ds744.2/docs/QSUG_v3.pdf

Dyer AJ. 1974. A review of flux-profile relations. *Boundary-Layer Meteorology* **1**: 363–372, DOI: 10.1007/BF00240838.

ECMWF, 2007. IFS DOCUMENTATION – Cy31r1, Operational implementation 12 September 2006, Part IV, Physical processes, 155. Retrieved October 17, 2012. Available at http://www.ecmwf.int/research/ifsdocs/CY31r1/index.html

Edson JB, Hinton AA, Prada KE, Hare JE, Fairall CW. 1998. Direct covariance flux estimates from mobile platforms at sea. *Journal of Atmospheric and Oceanic Technology* **15**: 547–562, DOI: 10.1175/1520-0426(1998)015<0547:DCFEFM>2.0.CO;2.

Fairall CW, Bradley EF, Rogers DP, Edson JB, Young GS. 1996. Bulk parameterization of air-sea fluxes for TOGA COARE. *Journal of Geophysical Research* **101**: 3747–3764, DOI: 10.1029/95JC03205.

Fairall CW, Bradley EF, Hare JE, Grachev AA, Edson JB. 2003. Bulk parameterization of air–sea fluxes: updates and verification for the COARE algorithm. *Journal of Climate* **16**: 571–591, DOI: 10.1175/1520- 0442(2003)016<0571:BPOASF>2.0.CO;2.

Fairall CW, Barnier B, Berry DI, Bourassa MA, Bradley F, Clayson CA, de Leeuw G, Drennan WM, Gille ST, Gulev SK, Kent EC, McGillis WR, Quartly GD, Ryabinin V, Smith SR, Weller RA, Yelland MJ, Zhang H-M. 2010. Observations to quantify air-sea fluxes and their role in climate variability and predictability. In *Proceedings of OceanObs'09: Sustained Ocean Observations and Information for Society*, Vol. **2** 21–25 September 2009, Hall J, Harrison DE, Stammer D (eds). ESA Publication WPP-306: Venice, Italy.

Fairall CW, Yang M, Bariteau L, Edson JB, Helmig D, McGillis W, Pezoa S, Hare JE, Huebert B, Blomquist B. 2011. Implementation of the coupled ocean-atmosphere response experiment flux algorithm with CO_2, dimethyl sulfide, and O_3. *Journal of Geophysical Research* **116**: C00F09, DOI: 10.1029/2010JC006884.

Fangohr S, Kent EC. 2012. An estimate of structural uncertainty in QuikSCAT wind vector retrievals. *Journal of Applied Meteorology and Climatology* **51**: 954–961, DOI: 10.1175/JAMC-D-11-0183.1.

Fangohr S, Woolf DK. 2007. Application of new parameterizations of gas transfer velocity and their impact on regional and global marine CO_2 budgets. *Journal of Marine Systems* **66**: 195–203, DOI: 10.1016/j.jmarsys.2006.01.012.

Fangohr S, Woolf DK, Jeffery CD, Robinson IS. 2008. Calculating long-term global air-sea flux of carbon dioxide using scatterometer, passive microwave, and model reanalysis wind data. *Journal of Geophysical Research* **113**: C09032, DOI: 10.1029/2005JC003376.

Fennig K, Andersson A, Bakan S, Klepp C-P, Schröder M, 2012. Hamburg Ocean Atmosphere Parameters and Fluxes from Satellite Data – HOAPS 3.2 – Monthly Means / 6-Hourly Composites. Satellite Application Facility on Climate Monitoring, DOI: 10.5676/EUM_SAF_CM/HOAPS/V001.

Gilhousen DB. 1987. A field evaluation of NDBC moored buoy winds. *Journal of Atmospheric and Oceanic Technology* **4**: 94–104, DOI: 10.1175/1520-0426(1987)004<0094:AFEONM>2.0.CO;2.

Glover DM, Frew NM, McCue SJ, Bock EJ. 2002. A multiyear time series of global gas transfer velocity from the TOPEX dual frequency, normalized radar backscatter algorithm. In *Gas Transfer at Water Surfaces. Geophysical Monograph*, Vol. **127**, Donelan MA, Drennan WM, Saltzman ES, Wanninkhof R (eds). AGU: Washington, DC; 325–331.

Gould WJ, Smith SR. 2006. Research vessels: underutilized assets for climate observations. *EOS: Transactions American Geophysical Union* **87**(22): 214–215, DOI: 10.1029/2006EO220003.

Gulev SK. 1997. Climatologically significant effects of space-time averaging in the North Atlantic sea-air heat flux fields. *Journal of Climate* **10**: 2743–2763, DOI: 10.1175/1520-0442(1997)010<2743:CSEOST>2.0.CO;2.

Gulev SK, Jung T, Ruprecht E. 2007. Estimation of the impact of sampling errors in the VOS observations on air-sea fluxes. Part I. Uncertainties in climate means. *Journal of Climate* **20**: 279–301, DOI: 10.1175/JCLI4010.1.

IFREMER/CERSAT, 2002a. Mean Wind Fields (MWF product) – User Manual – Volume 1 : ERS-1, ERS-2 & NSCAT, C2-MUT-W-05-IF, CERSAT - IFREMER, Version 1, April 2002, 54. Retrieved October 17, 2012. Available at ftp://ftp.ifremer.fr/ifremer/cersat/documentation/gridded/mwf-ers/mwf_vol1.pdf

IFREMER/CERSAT, 2002b. Mean Wind Fields (MWF product) – User Manual – Volume 2 : QuikSCAT, C2-MUT-W-04-IF, CERSAT - IFREMER, 48. Retrieved October 17, 2012. Available at ftp://ftp.ifremer.fr/ifremer/cersat/documentation/gridded/mwf-quikscat/mwf_vol2.pdf

Josey SA, Kent EC, Taylor PK. 1995. Seasonal variations between sampling and classical mean turbulent heat flux estimates in the North Atlantic. *Annales Geophysicae* **13**: 1054–1064, DOI: 10.1007/s00585-995-1054-3.

Kalnay E, Kanamitsu M, Kistler R, Collins W, Deaven D, Gandin L, Iredell M, Saha S, White G, Woolen J, Zhu Y, Chelliah M, Ebisuzaki W, Higgins W, Janowiak J, Mo KC, Ropelewski C, Wang J, Leetma A, Reynolds RW, Jenne R, Joseph D. 1996. The NCEP/NCAR 40-year reanalysis project. *Bulletin of the American Meteorological Society* **77**: 437–471, DOI: 10.1175/1520-0477(1996)077<0437:TNYRP>2.0.CO;2.

Kanamitsu M, Ebisuzaki W, Woollen J, Yang S-K, Hnilo JJ, Fiorino M, Potter GL. 2002. NCEP–DOE AMIP-II Reanalysis (R-2). *Bulletin of the American Meteorological Society* **83**: 1631–1643, DOI: 10.1175/BAMS-83-11-1631.

Kara AB, Wallcraft AJ, Barron CN, Hurlburt HE, Bourassa MA. 2008a. Accuracy of 10 m winds from satellites and NWP products near land-sea boundaries. *Journal of Geophysical Research* **113**: C10020, DOI: 10.1029/2007/JC004516.

Kara AB, Wallcraft AJ, Bourassa MA. 2008b. Air-sea stability effects on the 10 m winds over the global ocean: evaluations of air-sea flux algorithms. *Journal of Geophysical Research* **113**: C04009, DOI: 10.1029/2007JC004324.

Kent EC, Berry DI. 2005. Quantifying random errors in voluntary observing ships meteorological observations. *International Journal of Climatology* **25**(7): 843–856, DOI: 10.1002/joc.1167.

Kent EC, Challenor PG. 2006. Toward estimating climatic trends in SST, part 2: random errors. *Journal of Atmospheric and Oceanic Technology* **23**: 476–486, DOI: 10.1175/JTECH1844.1.

Kent EC, Taylor PK. 1995. A comparison of sensible and latent heat flux estimates for the North Atlantic Ocean. *Journal of Physical Oceanography* **25**: 1530–1549, DOI: 10.1175/1520-0485(1995)025<1530:ACOSAL>2.0.CO;2.

Kent EC, Taylor PK. 1997. Choice of a Beaufort equivalent scale. *Journal of Atmospheric and Oceanic Technology* **14**: 228–242, DOI: 10.1175/1520-0426(1997)014<0228:COABES>2.0.CO;2.

Kent EC, Taylor PK, Challenor PG. 1998. A comparison of ship and scatterometer-derived wind speed data in open ocean and coastal areas. *International Journal of Remote Sensing* **19**: 3361–3381, DOI: 10.1080/014311698214046.

Kent EC, Woodruff SD, Berry DI. 2007. Metadata from WMO Publication No 47 and an assessment of voluntary observing ships observation heights in ICOADS. *Journal of Atmospheric and Oceanic Technology* **24**: 214–234, DOI: 10.1175/JTECH1949.1.

Large WG, Pond S. 1981. Open ocean momentum flux measurements in moderate to strong winds. *Journal of Physical Oceanography* **11**: 324–336, DOI: 10.1175/1520-0485(1981)011<0324:OOMFMI>2.0.CO;2.

Ledvina DL, Young GS, Miller RA, Fairall CW. 1993. The effect of averaging on bulk estimates of heat and momentum fluxes for the tropical western Pacific Ocean. *Journal of Geophysical Research* **98**: 20211–20217, DOI: 10.1029/93JC01856.

Lee T, McPhaden MJ. 2008. Decadal phase change in large-scale sea level and winds in the Indo-Pacific region at the end of the 20th century. *Geophysical Research Letters* **35**: L01705, DOI: 10.1029/2007GL032419.

Lindau R. 1995. A new Beaufort Equivalent Scale. In *Proceedings of the International COADS Winds Workshop*, Kiel, Germany, Berichte aus dem Institut für Meereskunde, 232–252.

Liu WT, Katsaros KB, Businger JA. 1979. Bulk parameterization of air-sea exchanges of heat and water vapour including the molecular constraints at the interface. *Journal of the Atmospheric Sciences* **36**: 1722–1735, DOI: 10.1175/1520-0469(1979)036<1722:BPOASE>2.0.CO;2.

McPhaden MJ, Busalacchi AJ, Cheney R, Donguy J-R, Gage KS, Halpern D, Ji M, Julian P, Meyers G, Mitchum GT, Niiler PP, Picaut J, Reynolds RW, Smith N, Takeuchi K. 1998. The tropical ocean-global atmosphere (TOGA) observing system: a decade of progress. *Journal of Geophysical Research* **103**: 14 169–14 240, DOI: 10.1029/97JC02906.

McPhaden MJ, Meyers G, Ando K, Masumoto Y, Murty VSN, Ravichandran M, Syamsudin F, Vialard J, Yu L, Yu W. 2009. RAMA: the research moored array for African-Asian-Australian monsoon analysis and prediction. *Bulletin of the American Meteorological Society* **90**: 459–480, DOI: 10.1175/2008BAMS2608.1.

Mears CA, Smith DK, Wentz FJ. 2001. Comparison of Special Sensor Microwave Imager and buoy-measured wind speeds from 1987–1997. *Journal of Geophysical Research* **106**: 11 719–11 729, DOI: 10.1029/1999JC000097.

Meissner T, Smith D, Wentz F. 2001. A 10 year intercomparison between collocated Special Sensor Microwave Imager oceanic surface wind speed retrievals and global analyses. *Journal of Geophysical Research* **106**: 11 731–11 742, DOI: 10.1029/1999JC000098.

Melsheimer C, Alpers W, Gade M. 2001. Simultaneous observations of rain cells over the ocean by the synthetic aperture radar aboard the ERS satellites and by surface-based weather radars. *Journal of Geophysical Research* **106**: 4665–4678, DOI: 10.1029/2000JC000263.

Moat BI, Yelland MJ, Pascal RW, Molland AF. 2005. An overview of the airflow distortion at anemometer sites on ships. *International Journal of Climatology* **25**: 997–1006, DOI: 10.1002/joc.1177.

Nightingale PD, Malin G, Law CS, Watson AJ, Liss PS, Liddicoat MI, Boutin J, Upstill-Goddard RC. 2000. In situ evaluation of air-sea gas exchange parameterizations using novel conservative and volatile tracers. *Global Biogeochemical Cycles* **14**: 373–87, DOI: 10.1029/1999GB900091.

Offiler D. 1994. The calibration of ERS-1 satellite scatterometer winds. *Journal of Atmospheric and Oceanic Technology* **11**: 1002–1017, DOI: 10.1175/1520-0426(1994)011<1002:TCOSSW>2.0.CO;2.

Prytherch J, Yelland MJ, Pascal RW, Moat BI, Skjelvan I, Srokosz MA. 2010. Open ocean gas transfer velocity derived from long-term direct measurements of the CO_2 flux. *Geophysical Research Letters* **37**: L23607, DOI: 10.1029/2010GL045597.

Queffeulou P, Bentamy A, Lavergne T, Lefevre JM, Skandrani C, 2003. Mediterranean Sea wind and wave characteristics from satellite, buoy and numerical model data, *IGARSS 2003: IEEE International Geoscience And Remote Sensing Symposium*, Vols **I-VII:** Proceedings, 1924–1926, DOI: 10.1109/IGARSS.2003.1294294.

Rayner NA, Parker DE, Horton EB, Folland CK, Alexander LV, Rowell DP, Kent EC, Kaplan A. 2003. Global analyses of SST, sea ice and night marine air temperature since the late 19th century. *Journal of Geophysical Research* **108**(D14): 4407, DOI: 10.1029/2002JD002670.

Reynolds RW, Smith TM. 1994. Improved global sea surface temperature analyses using optimum interpolation. *Journal of Climate* **7**: 929–948, DOI: 10.1175/1520-0442(1994)007<0929:IGSSTA>2.0.CO;2.

Reynolds RW, Rayner NA, Smith TM, Stokes DC, Wang W. 2002. An improved *in situ* and satellite SST analysis for climate. *Journal of Climate* **15**: 1609–1625, DOI: 10.1175/1520-0442(2002)015<1609:AIISAS>2.0.CO;2.

Ricciardulli L, Wentz F, 2011. Reprocessed QuikSCAT (V04) wind vectors with Ku-2011 geophysical model function. Remote Sensing Systems Tech. Rep. 043011, 8. Retrieved October 17, 2012. Available at http://www.ssmi.com/qscat/qscat_Ku2011_tech_report.pdf

Rienecker MM, Suarez MJ, Gelaro R, Todling R, Bacmeister J, Liu E, Bosilovich MG, Schubert SD, Takacs L, Kim G-K, Bloom S, Chen J, Collins D, Conaty A, da Silva A, Gu W, Joiner J, Koster RD, Lucchesi R, Molod A, Owens T, Pawson S, Pegion P, Redder CR, Reichle R, Robertson FR, Ruddick AG, Sienkiewicz M, Woollen J. 2011. MERRA - NASA's modern-era retrospective analysis for research and applications. *Journal of Climate* **24**: 3624–3648, DOI: 10.1175/JCLI-D-11-00015.1.

Saha S, Moorthi S, Pan HL, Wu X, Wang J, Nadiga S, Tripp P, Kistler R, Woollen J, Behringer D, Liu H, Stokes D, Grumbin R, Gayno G, Wang J, Hou YT, Chuang HY, Juang HMH, Sela J, Iredell M, Treadon R, Kleist D, Delst PV, Keyser D, Derber J, Ek M, Meng J, Wei H, Yang R, Lord S, van den Dool HM, Kumar A, Wang W, Long C, Chelliah M, Xue Y, Huang B, Higgin W, Zou CZ, Liu Q, Chen Y, Han Y, Cucurull L, Reynolds RW, Rutledge G, Goldber M. 2010. The NCEP climate forecast system reanalysis. *Bulletin of the American Meteorological Society* **91**: 1015–1057, DOI: 10.1175/2010BAMS3001.1.

Smith SD. 1980. Wind stress and heat flux over the ocean in gale force winds. *Journal of Physical Oceanography* **10**: 709–726, DOI: 10.1175/1520- 0485(1980)010<0709:WSAHFO>2.0.CO;2.

Smith SD. 1988. Coefficients for sea surface wind stress, heat flux and wind profiles as a function of wind speed and temperature. *Journal of Geophysical Research* **93**: 15 467–15 472, DOI: 10.1029/JC093iC12p15467.

Smith SR, Bourassa MA, Sharp RJ. 1999. Establishing more truth in true winds. *Journal of Atmospheric and Oceanic Technology* **16**: 939–952, DOI: 10.1175/1520-0426(1999)016<0939:EMTITW>2.0.CO;2.

Smith SR, Hughes PJ, Bourassa MA. 2011. A comparison of nine monthly air–sea flux products. *International Journal of Climatology* **31**: 1002–1027, DOI: 10.1002/joc.2225.

Thomas BR, Kent EC, Swail VR. 2005. Methods to homogenize wind speeds from ships and buoys. *International Journal of Climatology* **25**(7): 979–995, DOI: 10.1002/joc.1176.

Thomas BR, Kent EC, Swail VR, Berry DI. 2008. Analysis of monthly mean marine winds adjusted for observation method and height. *International Journal of Climatology* **28**(6): 747–763, DOI: 10.1002/joc.1570.

Trenberth K, Dole R, Xue Y, Onogi K, Dee D, Balmaseda M, Bosilovich M, Schubert S, Large L. 2010. Atmospheric reanalyses: a major resource for ocean product development and modeling. In *Proceedings of OceanObs'09: Sustained Ocean Observations and Information for Society*, Vol. **2** 21–25 September 2009, Hall J,

Harrison DE, Stammer D (eds). ESA Publication WPP-306: Venice, Italy, DOI: 10.5270/OceanObs09.cwp.90.

Uppala SM, Kållberg PW, Simmons AJ, Andrae U, Bechtold VDC, Fiorino M, Gibson JK, Haseler J, Hernandez A, Kelly GA, Li X, Onogi K, Saarinen S, Sokka N, Allan RP, Andersson E, Arpe K, Balmaseda MA, Beljaars ACM, Berg LVD, Bidlot J, Bormann N, Caires S, Chevallier F, Dethof A, Dragosavac M, Fisher M, Fuentes M, Hagemann S, Hólm E, Hoskins BJ, Isaksen L, Janssen PAEM, Jenne R, Mcnally AP, Mahfouf J-F, Morcrette J-J, Rayner NA, Saunders RW, Simon P, Sterl A, Trenberth KE, Untch A, Vasiljevic D, Viterbo P, Woollen J. 2005. The ERA-40 reanalysis. *Quarterly Journal of the Royal Meteorological Society* **131**: 2961–3012, DOI: 10.1256/qj.04.176.

Uppala S, Dee D, Kobayashi S, Berrisford P, Simmons A. 2008a. Towards a climate data assimilation system: status update of ERA-Interim. *ECMWF Newsletter* **115**: 12–18.

Uppala S, Dee D, Kobayashi S, Simmons A, 2008b. Evolution of reanalysis at ECMWF. In *Proceeding of 3rd WCRP International Conference on Reanalysis*, Tokyo, Japan. Retrieved October 17, 2012. Available at http://wcrp.ipsl.jussieu.fr/Workshops/Reanalysis2008/Documents/V1-102_ea.pdf.

Verhoef A, Stoffelen A, 2011. ASCAT Wind Product User Manual version 1.10, SAF/OSI/CDOP/KNMI/TEC/MA/126, EUMETSAT. Retrieved October 17, 2012. Available at http://www.knmi.nl/publications/fulltexts/ss3_pm_ascat_1.10.pdf)

Wallcraft AJ, Kara AB, Barron CN, Metzger EJ, Pauley RL, Bourassa MA. 2009. Comparison of monthly mean 10 m wind speeds from satellite and NWP products over the global ocean. *Journal of Geophysical Research* **114**: D16109, DOI: 10.1029/2008JD011696.

Wanninkhof R. 1992. Relationship between gas exchange and wind speed over the ocean. *Journal of Geophysical Research.* **97**: 7373–81, DOI: 10.1029/92JC00188.

Wanninkhof R, Doney SC, Takahashi T, McGillis WR. 2002. The effect of using averaged winds on global air–sea CO_2 fluxes. In *Gas Transfer at Water Surfaces. Geophysical Monograph*, Vol. **127**, Donelan MA, Drennan WM, Saltzman ES, Wanninkhof R (eds). AGU: Washington, DC; 351–356.

Wanninkhof R, Asher WE, Ho DT, Sweeney C, McGillis WR. 2009. Advances in quantifying air-sea gas exchange and environmental forcing. *Annual Review of Marine Science* **1**: 213–244, DOI: 10.1146/annurev.marine.010908.163742.

WCRP, 1989. WOCE Surface Flux Determinations – A strategy for *in situ* measurements. Working Group on *in situ* measurements for Fluxes WCRP-23 (WMO/TD No.304), WMO, Geneva.

Webster PA, Lukas R. 1992. The coupled ocean–atmosphere response experiment. *Bulletin of the American Meteorological Society* **73**: 1377–1416, DOI: 10.1175/1520-0477(1992)073<1377:TCTCOR>2.0.CO;2.

Weller RA, Bradley EF, Lukas R. 2004. The interface or air-sea flux component of the TOGA Coupled Ocean–atmosphere Response Experiment and its impact on subsequent air-sea interaction studies. *Journal of Atmospheric and Oceanic Technology* **21**: 223–257, DOI: 10.1175/1520-0426(2004)021<0223:TIOAFC>2.0.CO;2.

Weller RA, Bradley EF, Edson JB, Fairall CW, Brooks I, Yelland MY, Pascal RW. 2008. Sensors for physical fluxes at the sea surface: energy, heat, water, salt. *Ocean Science* **4**(4): 247–263, DOI: 10.5194/os-4-247-2008.

WGASF, 2000 Intercomparison and validation of ocean–atmosphere energy flux fields - Final report of the Joint WCRP/SCOR Working Group on Air-Sea Fluxes. WCRP-112, WMO/TD-1036. Taylor PK (ed). 306 pp. Retrieved October 17, 2012. Available at http://eprints.soton.ac.uk/69522/

Woodruff SD, Diaz HF, Elms JD, Worley SJ. 1998. COADS Release 2 data and metadata enhancements for improvements of marine surface flux fields. *Physics and Chemistry of the Earth* **23**: 517–526.

Woodruff SD, Diaz HF, Kent EC, Reynolds RW, Worley SJ. 2008. The evolving SST record from ICOADS. In *Advances in Global Change Research*, Vol. **33** Climate Variability and Extremes During the Past 100 Years, Brönnimann S, Luterbacher J, Ewen T, Diaz HF, Stolarski RS, Neu U (eds). Springer: The Netherlands, 364 pp.

Woodruff SD, Worley SJ, Lubker SJ, Ji Z, Freeman JE, Berry DI, Brohan P, Kent EC, Reynolds RW, Smith SR, Wilkinson C. 2011. ICOADS release 2.5 and data characteristics. *International Journal of Climatology* **31**(7): 951–967, DOI: 10.1002/joc.2103.

Woolf DK. 2005. Parameterization of gas transfer velocities and seastate dependent wave breaking. *Tellus* **57B**: 87–94, DOI: 10.1111/j.1600-0889.2005.00139.x.

Worley SJ, Woodruff SD, Reynolds RW, Lubker SJ, Lott N. 2005. ICOADS Release 2.1 data and products. *International Journal of Climatology* **25**: 823–842, DOI: 10.1002/joc.1166.

Yelland MJ, Moat BI, Pascal RW, Berry DI. 2002. CFD model estimates of the airflow distortion over research ships and the impact on momentum flux measurements. *Journal of Atmospheric and Oceanic Technology* **19**: 1477–1499, DOI: 10.1175/1520-0426(2002)019<1477:CMEOTA>2.0.CO;2.

Yu L, O'Brien JJ. 1991. Variational estimation of the wind stress drag coefficient and the oceanic eddy viscosity profile. *Journal of Physical Oceanography* **21**: 709–719, DOI: 10.1175/1520-0485(1991)021<0709:VEOTWS>2.0.CO;2.

Yu L, O'Brien JJ. 1995. Variational data assimilation for determining the seasonal net surface heat flux using a tropical Pacific Ocean model. *Journal of Physical Oceanography* **25**: 2319–2343, DOI: 10.1175/1520-0485(1995)025<2319:VDAFDT>2.0.CO;2.

Yu L, Weller RA. 2007. Objectively analyzed air-sea heat fluxes for the global ice-free oceans (1981–2005). *Bulletin of the American Meteorological Society* **88**: 527–539, DOI: 10.1175/BAMS-88-4-527.

Yu L, Weller RA, Sun B. 2004. Improving latent and sensible heat flux estimates for the Atlantic Ocean (1988–1999) by a synthesis approach. *Journal of Climate* **17**: 373–393, DOI: 10.1175/1520-0442(2004)017<0373:ILASHF>2.0.CO;2.

Yu L, Jin X, Weller RA, 2008. Multidecade Global Flux Datasets from the Objectively Analyzed Air-sea Fluxes (OAFlux) Project: Latent and sensible heat fluxes, ocean evaporation, and related surface meteorological variables. Woods Hole Oceanographic Institution, OAFlux Project Technical Report. OA-2008-01, 64. Woods Hole. Massachusetts. Retrieved October 17, 2012. Available at http://oaflux.whoi.edu/pdfs/OAFlux_TechReport_3rd_release.pdf

Zeng L, Levy G. 1995. Space and time aliasing structure in monthly mean polar orbiting satellite data. *Journal of Geophysical Research* **100**(D3): 5133–5142, DOI: 10.1029/94JD03252.

Zhang H-M, Bates JJ, Reynolds RW. 2006a. Assessment of composite global sampling: sea surface wind speed. *Geophysical Research Letters* **33**: L17714, DOI: 10.1029/2006GL027086.

Zhang H-M, Reynolds RW, Bates JJ, 2006b. Blended and Gridded High Resolution Global Sea Surface Wind Speed and Climatology from Multiple Satellites: 1987 – Present, American Meteorological Society 2006 Annual Meeting, Paper #P2.23, Atlanta, GA.